*J. Fluid Mech.* (1997), *vol.* 333, *pp.* 327–373



# Reappraisal of the Kelvin–Helmholtz problem. Part 2. Interaction of the Kelvin–Helmholtz, superharmonic and Benjamin–Feir instabilities

By T. BROOKE BENJAMIN[1]† AND THOMAS J. BRIDGES[2]

[1]Mathematical Institute, Oxford University, 24-29 St. Giles, Oxford OX1 3LB, UK

[2]Department of Mathematical and Computing Sciences, University of Surrey, Guildford, Surrey GU2 5XH, UK

(Received 3 May 1996 and in revised form 12 September 1996)

Several new results on the bifurcation and instability of nonlinear periodic travelling waves, at the interface between two fluids in relative motion, in a parametric neighbourhood of a Kelvin–Helmholtz unstable equilibrium are presented. The organizing centre for the analysis is a canonical Hamiltonian formulation of the Kelvin–Helmholtz problem presented in Part 1. When the density ratio of the upper and lower fluid layers exceeds a critical value, and surface tension is present, a pervasive superharmonic instability is found, and as $u \to u_0$, where $u$ is the velocity difference between the two layers and $u_0$ is the Kelvin–Helmholtz threshold, the amplitude at which the superharmonic instability occurs scales like $(u_0 - u)^{1/2}$ with $u < u_0$. Other results presented herein include (*a*) new results on the structure of the superharmonic instability, (*b*) the discovery of isolated branches and intersecting branches of travelling waves near a critical density ratio, (*c*) the appearance of Benjamin–Feir instability along branches of waves near the Kelvin–Helmholtz instability threshold and (*d*) the interaction between the Kelvin–Helmholtz, superharmonic and Benjamin–Feir instability at low amplitude.

## 1. Introduction

In Part 1 (Benjamin & Bridges 1997), a new Hamiltonian structure for the Kelvin–Helmholtz problem for both a single-valued interface and an overhanging multi-valued or breaking interface, as well as the implications for conservation laws and the linearized Kelvin–Helmholtz (KH) problem, were presented. In this paper the implications of the Hamiltonian formulation for the bifurcation and stability of nonlinear travelling waves (TWs) near a KH unstable equilibrium are studied. The finite-amplitude TWs and their instabilities near the KH threshold are likely to provide a backbone for the complex roll-up, leading to interfacial wave-breaking and a complicated mixing layer, which is observed in experiments and numerical simulations (cf. Drazin & Reid 1981, §1.4). One of the results of the analysis of TWs in this paper is the discovery of a pervasive superharmonic (SH) instability of finite-amplitude TWs, which coalesces with the KH unstable equilibrium and is a potential mechanism for interfacial wave breaking and KH roll-up, before the KH threshold. Other new results to be presented include (*a*) for *all* density ratios exceeding a critical value, the positive-energy and negative-energy TWs are globally

† TBB (1929–1995) *requiescat in pace.*

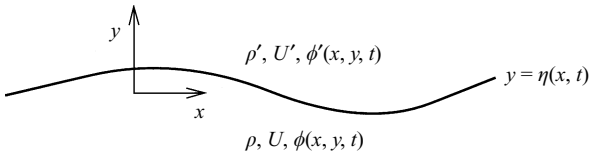


FIGURE 1. Schematic of the interfacial wave problem.

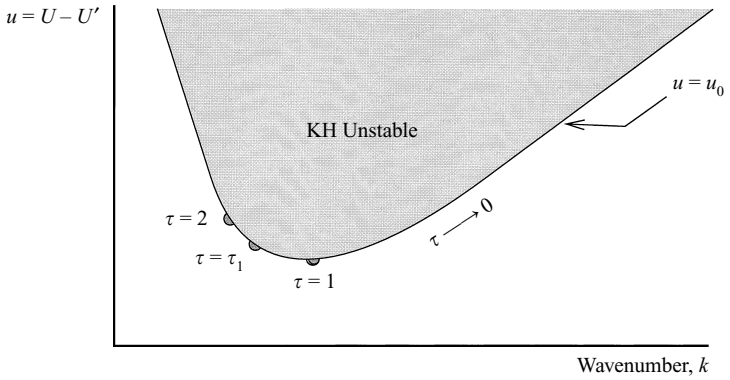


FIGURE 2. Neutral curve for KH instability. The parameter $\tau$ is defined in §2.

connected and this connected branch has both a Benjamin–Feir (BF) instability and an SH instability at low amplitudes. (*b*) In the neighbourhood of a critical density ratio, the negative-energy and positive-energy TWs intersect transversely (see figure 16) with a change of SH stability precisely at the bifurcation point. (*c*) Saffman's theory for the SH instability is extended in order to determine whether positive or negative slope, in the energy–wave speed diagram, corresponds to SH instability. It is found that both positive and negative slopes may correspond to instability; further information, which is available within the Hamiltonian formulation, is used to determine precisely which slope corresponds to instability (cf. §§3.1, 3.2 and Appendix B). (*d*) A novel interaction between the KH unstable equilibrium, and the SH and BF instabilities of a nearby TW branch (see figure 4). In addition to their importance for insight into the nonlinear KH problem, the results presented here are also of basic interest for understanding the SH instability since it occurs at low amplitude in the KH problem, in contrast with the classic water-wave problem, and can be studied, in some completeness, analytically.

A schematic of the interfacial wave problem is shown in figure 1. The neutral curve for the linearized KH problem – when surface tension is present – is shown in figure 2. The equation for the neutral curve will be given below. The parameters $\rho$ and $U$ and $\rho'$ and $U'$ correspond to the constant densities and velocities in the lower (unprimed) and upper (primed) fluid layers and

$$u \stackrel{\text{def}}{=} U - U' \quad \text{and} \quad r \stackrel{\text{def}}{=} \frac{\rho - \rho'}{\rho + \rho'}.$$

The first nonlinear analysis of the KH problem is in the work of Drazin (1970). Using a Stuart-Watson expansion, an ordinary differential equation model for the bifurcation and stability of weakly nonlinear TWs was derived. In fact the instability predicted by Drazin's model equation is precisely an SH instability. Further aspects of this model are considered in §2.4. Nayfeh & Saric (1972) derive the first space-

time modulation equation for the KH problem valid in the neighbourhood of the neutral curve in figure 2 away from resonances and the minimum point. Weissman (1979) gives a comprehensive treatment including a multiple-scaling analysis in two space dimensions and time and shows that a complex Klein–Gordon equation is the appropriate modulation equation near the minimum point of the neutral curve in figure 2. Some analysis of this modulation equation was presented by Weissman, including exact solutions for kinks and pulses and a numerical study of the initial-value problem, but surprisingly, the sideband instability of TWs was not considered (see §4.2 for further discussion). Miles (1986) presented the first Lagrangian analysis of the KH problem and recovered the previous results of Drazin (1970) and Nayfeh & Saric (1972). There has also been a number of numerical studies of aspects of the the KH problem including roll-up (cf. Yuen 1984; Bontozoglou & Hanratty 1988 and the references in Drazin & Reid 1981, §1.4 and Part 1) as well as numerical studies of sideband instabilities (cf. Yuen 1984; Pullin & Grimshaw 1985). The experiments of Thorpe (1969, 1978) show substantial agreement between the theoretical predictions of the KH theory and experiments with immiscible fluids. In Bridges, Christodoulides & Dias (1995) the spatial bifurcations of interfacial waves are considered with $U = U' = 0$ and surprisingly the bifurcation structure of the TWs, when considered as functions of the wavenumber, is similar to that found for the nonlinear TWs near the KH instability. In Dias & Bridges (1994) the Hamiltonian formulation of Part 1 is used to study the interaction between interfacial standing waves and TWs.

In this paper the nonlinear TWs near a KH unstable equilibrium are studied from a Hamiltonian perspective as follows. Let $\eta(x,t)$ be the interfacial wave height and define

$$\Phi(x,t) = \phi(x,y,t)\Big|_{y=\eta(x,t)} \quad \text{and} \quad \Phi'(x,t) = \phi'(x,y,t)\Big|_{y=\eta(x,t)} \tag{1.1}$$

where $\phi$ and $\phi'$ are the velocity potentials in the lower and upper fluid layers respectively. Throughout this paper the fluid layers will be taken to be infinite in extent. Define

$$\zeta(x,t) = \rho\Phi(x,t) - \rho'\Phi'(x,t)\,. \tag{1.2}$$

Then the main result of §3 of Benjamin & Bridges (1997, hereafter denoted by I), is that the governing equations for the KH problem are completely characterized by the canonical Hamiltonian representation

$$\frac{\partial}{\partial t}\begin{pmatrix}\eta\\ \zeta\end{pmatrix} = \begin{bmatrix}0 & 1\\ -1 & 0\end{bmatrix}\begin{pmatrix}\delta H/\delta\eta\\ \delta H/\delta\zeta\end{pmatrix} \tag{1.3}$$

where $H(\eta,\zeta)$ is the total disturbance energy. The novelty of (1.3) is that the potentials $\phi$ and $\phi'$ do not appear independently but only their boundary values constrained in the form (1.2). For periodic TWs the dependent variables are expanded in Fourier series,

$$\left.\begin{aligned}\eta(x,t) &= \sum_{n=1}^{\infty} A_n(t)\cos nkx + B_n(t)\sin nkx,\\ \zeta(x,t) &= \tfrac{1}{2}C_0(t) + \sum_{n=1}^{\infty} C_n(t)\cos nkx + D_n(t)\sin nkx\,,\end{aligned}\right\} \tag{1.4}$$

where the average of $\eta$ is set to zero. The analysis throughout the paper will be based on an $N$-term approximation of the Fourier series (1.4).

For any fixed $N$ let $\boldsymbol{X}(t) = (\boldsymbol{X}_1(t),\ldots,\boldsymbol{X}_N(t)) \in \mathbb{R}^{4N}$ with

$$\boldsymbol{X}_n(t) = (A_n(t), B_n(t), C_n(t), D_n(t)) \in \mathbb{R}^4\,, \quad t \in \mathbb{R}\,.$$

Then the object of §2.1 of the present paper is to reduce (1.3), for arbitrary but finite $N$, to the finite-dimensional Hamiltonian system

$$\boldsymbol{X}_t = \boldsymbol{J}_N \nabla H(\boldsymbol{X}), \quad \boldsymbol{X}(t) \in \mathbb{R}^{4N} \tag{1.5}$$

where $H(\boldsymbol{X})$ is the total (disturbance) energy evaluated on the finite Fourier series and $\boldsymbol{J}_N$ is a standard symplectic operator on $\mathbb{R}^{4N}$. The difficulty with the reduction from (1.3) to (1.5) is that the functional dependence of the energy on $\zeta$ is not apparent. The variational principle of I, §3.1 proves that the energy depends on $\zeta$ and provides an explicit and constructive method for obtaining this dependence.

Before proceeding to the nonlinear problem, an analysis of a single-mode approximation to the KH problem is instructive. It indicates how the variational principle of I, §3.1 generates a non-degenerate symplectic structure and also relates the KH instability to a classic – collision of imaginary eigenvalues of opposite Krein signature – instability in Hamiltonian systems. A single-mode approximation for the interfacial position $\eta(x,t)$, satisfying the linearized equations, is

$$\eta(x,t) = q_1(t)\cos kx + q_2(t)\sin kx \tag{1.6}$$

where $k$ is a fixed wavenumber. For the velocity potentials in the lower and upper layers let

$$\left.\begin{aligned} \phi(x,y,t) &= \mathrm{e}^{ky}[e_1(t)\cos kx + f_1(t)\sin kx], \\ \phi'(x,y,t) &= \mathrm{e}^{-ky}[e'_1(t)\cos kx + f'_1(t)\sin kx]\,. \end{aligned}\right\} \tag{1.7}$$

The functions $\phi$ and $\phi'$ are harmonic in the lower and upper fluid layers respectively and satisfy the far-field boundary conditions. It remains to satisfy the (linearized) boundary conditions at the interface (Drazin & Reid 1981, p. 17; I §2)

$$\left.\begin{aligned} \rho\eta_t + \rho U\eta_x - \rho\phi_y &= 0 \\ \rho'\eta_t + \rho' U'\eta_x - \rho\phi'_y &= 0 \\ \rho(\phi_t + U\phi_x) - \rho'(\phi'_t + U'\phi'_x) + (\rho-\rho')g\eta - \sigma\eta_{xx} &= 0 \end{aligned}\right\} \text{ at } y = 0 \tag{1.8}$$

where $g$ and $\sigma$ are the coefficients of gravity and surface tension respectively.

Substitution of (1.6) and (1.7) into (1.8) results in the following six ordinary differential equations:

$$\begin{aligned} \rho\frac{\mathrm{d}e_1}{\mathrm{d}t} - \rho'\frac{\mathrm{d}e'_1}{\mathrm{d}t} + \rho kUf_1 - \rho' U'kf'_1 + [(\rho-\rho')g + \sigma k^2]q_1 &= 0, \\ \rho\frac{\mathrm{d}f_1}{\mathrm{d}t} - \rho'\frac{\mathrm{d}f'_1}{\mathrm{d}t} - \rho kUe_1 + \rho' U'ke'_1 + [(\rho-\rho')g + \sigma k^2]q_2 &= 0, \\ \rho\frac{\mathrm{d}q_1}{\mathrm{d}t} + \rho kUq_2 - \rho ke_1 &= 0, \\ \rho\frac{\mathrm{d}q_2}{\mathrm{d}t} - \rho kUq_1 - \rho kf_1 &= 0, \\ \rho'\frac{\mathrm{d}q_1}{\mathrm{d}t} + \rho' kU'q_2 + \rho' ke'_1 &= 0, \\ \rho'\frac{\mathrm{d}q_2}{\mathrm{d}t} - \rho' kU'q_1 + \rho' kf'_1 &= 0\,, \end{aligned}$$

which can be recast into the interesting form

$$\boldsymbol{K}\boldsymbol{Z}_t = \nabla H(\boldsymbol{Z}) \tag{1.9}$$

with

$$\boldsymbol{Z} = \begin{pmatrix} q_1 \\ q_2 \\ e_1 \\ f_1 \\ e_1' \\ f_1' \end{pmatrix} \quad \text{and} \quad \boldsymbol{K} = \begin{bmatrix} \mathbf{0} & -\rho \boldsymbol{I}_2 & \rho' \boldsymbol{I}_2 \\ \rho \boldsymbol{I}_2 & \mathbf{0} & \mathbf{0} \\ -\rho' \boldsymbol{I}_2 & \mathbf{0} & \mathbf{0} \end{bmatrix}.$$

The function $H(\boldsymbol{Z})$ is the quadratic part of the total (disturbance) energy for the system evaluated on the single-mode solution (1.6) and (1.7) (cf. §2, (2.2) and (2.3)); that is, $H = K + V$, with $K$ the (disturbance) kinetic and $V$ the potential energy and

$$\left.\begin{aligned} K &= \tfrac{1}{2}\rho k(e_1^2 + f_1^2) + \tfrac{1}{2}\rho' k(e_1'^2 + f_1'^2) - \rho U k(e_1 q_2 - f_1 q_1) + \rho' U' k(q_2 e_1' - q_1 f_1'), \\ V &= \tfrac{1}{2}[(\rho - \rho')g + \sigma k^2](q_1^2 + q_2^2). \end{aligned}\right\} \tag{1.10}$$

The system (1.9) is a Hamiltonian system in a generalized sense. The operator $\boldsymbol{K}$ is skew-symmetric but it is not invertible (it has a two-dimensional kernel). The degeneracy arises because the kinetic energy depends on too many variables. This degeneracy can be eliminated by using the variational principle of I, §3.1. Let

$$\zeta(x,t) = p_1(t)\cos kx + p_2(t)\sin kx. \tag{1.11}$$

Then the constraint $[\rho\phi - \rho'\phi']|_{y=0} = \zeta$ for the single-mode approximation is

$$\rho e_1 - \rho' e_1' = p_1, \qquad \rho f_1 - \rho' f_1' = p_2. \tag{1.12}$$

In the single-mode setting the variational principle of I §3.1 is then

$$\mathscr{K}(\boldsymbol{q},\boldsymbol{p}) = \min K(e_1, f_1, e_1', f_1', q) \text{ subject to the constraint (1.12)}$$

with $\boldsymbol{q} : \mathbb{R} \to \mathbb{R}^2$ fixed. This is an elementary constrained variational problem on $\mathbb{R}^4$ with unique solution

$$\begin{pmatrix} e_1 \\ f_1 \\ e_1' \\ f_1' \end{pmatrix} = \frac{1}{\rho + \rho'} \begin{pmatrix} p_1 \\ p_2 \\ -p_1 \\ -p_2 \end{pmatrix} + \frac{U - U'}{\rho + \rho'} \begin{pmatrix} \rho' q_2 \\ -\rho' q_1 \\ \rho q_2 \\ -\rho q_1 \end{pmatrix}. \tag{1.13}$$

In other words, the variational principle leads to a transformation from $(e_1, f_1, e_1', f_1', \boldsymbol{q})$ to $(\boldsymbol{q},\boldsymbol{p})$ that reduces the overspecified system on $\mathbb{R}^6$ to a standard Hamiltonian system on $\mathbb{R}^4$. In terms of the transformed variables $(\boldsymbol{q},\boldsymbol{p})$ the Hamiltonian function for the system is

$$H = \frac{1}{2}\frac{k}{\rho + \rho'}(p_1^2 + p_2^2) + k c_0(p_2 q_1 - p_1 q_2) + \frac{1}{2}\frac{\rho\rho' k}{\rho + \rho'}(u_0^2 - u^2)(q_1^2 + q_2^2) \tag{1.14}$$

where

$$c_0 = \frac{\rho U + \rho' U'}{\rho + \rho'}, \quad u_0^2 = \frac{\rho + \rho'}{\rho\rho' k}(\sigma k^2 + (\rho - \rho')g) \quad \text{and} \quad u = U - U'. \tag{1.15}$$

Note that $H$ is again the quadratic part of the total (disturbance) energy but in terms of the new coordinates. The governing equations for the single-mode linear approximation are then

$$\dot{q}_j = \frac{\partial H}{\partial p_j} \quad \text{and} \quad \dot{p}_j = -\frac{\partial H}{\partial q_j} \quad j = 1, 2$$

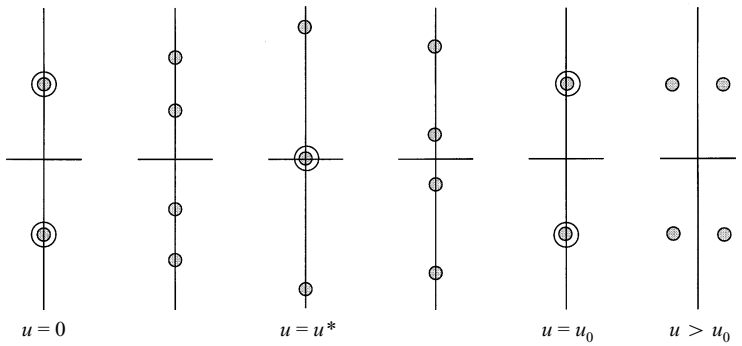


FIGURE 3. Schematic of the eigenvalue position in the complex $\lambda$-plane for the linear Hamiltonian system (1.14), as a function of $u = U - U'$ when $U' = 0$. The KH instability corresponds to $u > u_0$.

or

$$\frac{\mathrm{d}}{\mathrm{d}t}\begin{pmatrix} q_1 \\ q_2 \\ p_1 \\ p_2 \end{pmatrix} = \begin{bmatrix} 0 & -kc_0 & \dfrac{k}{\rho+\rho'} & 0 \\ kc_o & 0 & 0 & k\rho+\rho' \\ -\dfrac{\rho\rho' k}{\rho+\rho'}(u_0^2-u^2) & 0 & 0 & -kc_0 \\ 0 & -\dfrac{\rho\rho' k}{\rho+\rho'}(u_0^2-u^2) & kc_0 & 0 \end{bmatrix}\begin{pmatrix} q_1 \\ q_2 \\ p_1 \\ p_2 \end{pmatrix}.$$

With the ansatz $(\boldsymbol{q}, \boldsymbol{p}) = \mathrm{e}^{\lambda t}(\hat{\boldsymbol{q}}, \hat{\boldsymbol{p}})$ the eigenvalues of the above linear system are

$$\lambda = \pm \mathrm{i}\left(kc_0 \pm \frac{k}{\rho+\rho'}\left[\rho\rho'(u_0^2-u^2))\right]^{1/2}\right). \tag{1.16}$$

The positions of the eigenvalues (1.16) in the complex $\lambda$-plane are shown in figure 3 as a function of $u$ for the case $U' = 0$. Note that at some intermediate value of $u$ (denoted $u^*$) two eigenvalues pass through the origin but do not destabilize. Figure 3 shows that the KH instability corresponds, in the Hamiltonian setting, to a collision of eigenvalues of opposite Krein signature (opposite energy sign) on the imaginary axis. This instability has been well-studied in the Hamiltonian mechanics literature. The most well-known example of an instability of this type is the instability of the Lagrange equilibrium points in the restricted 3-body problem (cf. Deprit & Henrard 1968). A normal-form theory for the nonlinear problem near such an instability has been developed by van der Meer (1985) and named Hamiltonian Hopf bifurcation. A theory for bifurcation and stability of nonlinear periodic solutions near such an instability, including degeneracies and an example of a spinning double pendulum, is given in Bridges (1990, 1991). Some of the these results will be appealed to when analysing the nonlinear bifurcating TWs near the KH instability in §2.

The critical value of $u_0$ as a function of wavenumber $k$ is shown in figure 2 recovering the usual hydrodynamic neutral curve for the KH instability (cf. Weissman 1979, figure 1). The annotation along the neutral curve will be discussed in §2.

As shown in I, §5 and figure 3, the KH instability corresponds to a collision of modes of opposite energy sign. In §2 the nonlinear TWs emanating from these modes of opposite energy sign are studied. Depending on the density ratio, these waves may or may not interact at finite amplitude, and when they do interact there are interesting implications for the stability along the branch. A critical value of the

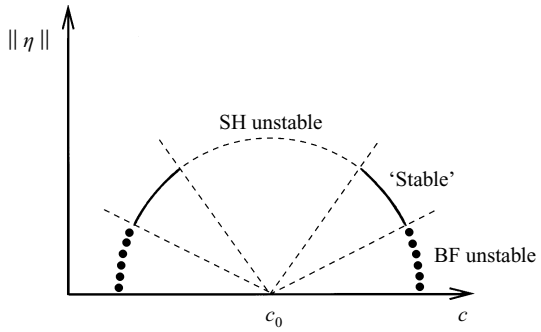


FIGURE 4. Globally connected positive- and negative-energy TWs for $r > r_0$ and $u < u_0$ and their stability assignments.

density ratio is also studied and complicated bifurcations of TWs are found as well as isolated branches of TWs above the KH unstable equilibrium.

The SH instability of TWs near the KH unstable equilibrium is studied in §3. The SH instability for the classic water-wave problem was first investigated by Longuet-Higgins (1978). Tanaka (1983, 1985) discovered in numerical calculations the connection between the SH instability and the energy maximum for TWs. Saffman (1985) gave an analytic proof, based on the Zakharov Hamiltonian formulation for water waves, that a maximum (or minimum) of energy corresponds to a change in SH stability. Recent work on SH instability has focused on the connection between SH instability and wave breaking (cf. Tanaka *et al.* 1987; Jillians 1989; Longuet-Higgins & Cleaver 1994). In the numerical study of Jillians (1989), all SH unstable modes investigated led to wave breaking.

In the present work, a pervasive SH instability is found at low amplitudes near (but before: $u < u_0$) the KH unstable equilibrium with an amplitude scaling like $(u_0 - u)^{1/2}$ as $u \to u_0$. Therefore, since SH instability has been shown to lead to wave breaking in the classic water-wave problem, and KH roll-up is a form of wave breaking, it is natural to propose SH instability as a new mechanism for the formation of KH billows. We do not argue that this is the only – or even the predominant – mechanism: indeed, a vortex sheet model explains roll-up quite adequately (cf. Saffman 1992, Chap. 8). However, the SH instability occurs for $u < u_0$, at low amplitude, and for a wide range of parameters and therefore provides a new mechanism for roll-up, before the KH threshold. It also includes the physically important effect of interfacial tension. In the experiments of Thorpe (1978), interfacial wave breaking was observed before the KH threshold but there is insufficient evidence to determine if SH instability is the mechanism there. In a similar vein, there are experimentally observed cases in which a free mixing layer, which is stable according to the linear stability criterion of Miles & Howard (minimum Richardson number exceeding $\frac{1}{4}$), is induced to undergo turbulent collapse (Drazin & Reid 1981, §44.3).

The BF instability also plays a role near the KH threshold, but does not seem to be as pervasive. A comprehensive treatment of BF instability of the TWs found here will not be given but a particularly interesting case is treated in some detail (see figure 4 and §4). When $r = (\rho - \rho')/(\rho + \rho') > r_0$, where $r_0$ is a critical value of $r$ and $u < u_0$, the bifurcating TWs are globally connected as shown in figure 4 (details in §§2–4). Figure 4 shows a branch of TWs in the $(c, \|\eta\|)$-plane, where $c$ is the phase speed and $\|\eta\|$ is the wave amplitude. The positive- and negative-energy TWs connect exactly at finite amplitude. As $u \to u_0$ this branch collapses into zero amplitude (noting that

zero amplitude represents the KH unstable equilibrium). A surprising result is that, for low amplitude, both the positive- and negative-energy TWs are BF unstable but stabilize and then lose stability at finite (but small) amplitude to an SH instability. The intermediate 'stable' region is in quotes since it is BF and SH stable but may be unstable to other classes of disturbances. The bifurcation and stability structure in figure 4 exists for a large region in parameter space near the KH threshold. The detailed verification of figure 4 is given in §4.

## 2. KH instability, TWs and bifurcations

The governing equations for the KH problem can be found in Drazin & Reid (1981, p. 17) and I, §2. The starting point of this section is the result of I, §3, that the governing equations take the following Hamiltonian form:

$$\frac{\partial}{\partial t}\begin{pmatrix}\eta\\ \zeta\end{pmatrix}=\begin{pmatrix}0 & 1\\ -1 & 0\end{pmatrix}\begin{pmatrix}\delta H/\delta\eta\\ \delta H/\delta\zeta\end{pmatrix}. \tag{2.1}$$

The Hamiltonian function is the total disturbance energy $H=K+V$ and on a space of $\ell$-periodic functions the potential energy is

$$V=\frac{2}{\ell}\int_0^{\ell}\left\{\tfrac{1}{2}(\rho-\rho')g\eta^2+\sigma\left(\left(1+\eta_x^2\right)^{1/2}-1\right)\right\}\mathrm{d}x. \tag{2.2}$$

The kinetic energy is composed of two parts, $K=K_1+K_2$, with

$$\left.\begin{aligned}K_1&=\frac{2}{\ell}\int_0^{\ell}\left\{\int_{-\infty}^{\eta}\tfrac{1}{2}\rho|\nabla\phi|^2\mathrm{d}y+\int_{\eta}^{\infty}\tfrac{1}{2}\rho'|\nabla\phi'|^2\mathrm{d}y\right\}\mathrm{d}x,\\ K_2&=\frac{2}{\ell}\int_0^{\ell}\left\{-\rho U\Phi+\rho' U'\Phi'\right\}\eta_x\,\mathrm{d}x,\end{aligned}\right\} \tag{2.3}$$

(cf. I, §3.1). The symplectic form for the system is

$$\Omega=\frac{2}{\ell}\int_0^{\ell}(\,\mathrm{d}\zeta\wedge\mathrm{d}\eta\,)\,\mathrm{d}x. \tag{2.4}$$

In this section the KH problem will be reduced to a finite-dimensional Hamiltonian system by expanding $\eta$ and $\zeta$ in Fourier series. Fixing the mean interfacial elevation to be zero, the finite Fourier series expansions take the form

$$\left.\begin{aligned}\eta(x,t)&=\sum_{n=1}^{N}A_n(t)\cos nkx+B_n(t)\sin nkx,\\ \zeta(x,t)&=\tfrac{1}{2}C_0(t)+\sum_{n=1}^{N}C_n(t)\cos nkx+D_n(t)\sin nkx,\end{aligned}\right\} \tag{2.5}$$

where $k=2\pi/\ell$. Introduce the $4N$-vector of $t$-dependent Fourier coefficients

$$\boldsymbol{X}(t)=\begin{pmatrix}\boldsymbol{X}_1(t)\\ \vdots\\ \boldsymbol{X}_N(t)\end{pmatrix}\in\mathbb{R}^{4N}\quad\text{with}\quad\boldsymbol{X}_n(t)=\begin{pmatrix}A_n(t)\\ B_n(t)\\ C_n(t)\\ D_n(t)\end{pmatrix},\quad n=1,\ldots,N. \tag{2.6}$$

The system (2.1) will be reduced to a finite-dimensional Hamiltonian system of the form

$$\boldsymbol{X}_t=\boldsymbol{J}_N\nabla H(\boldsymbol{X}),\qquad\boldsymbol{X}(t)\in\mathbb{R}^{4N} \tag{2.7}$$

where $N$ is arbitrary but finite. The operator $\boldsymbol{J}_N$ is a standard symplectic operator in the sense that $\boldsymbol{J}_N^{-1} = \boldsymbol{J}_N^T = -\boldsymbol{J}_N$ and $H$ is the disturbance energy of the KH problem restricted to the finite Fourier series.

The difficulty with this reduction is that the kinetic energy apparently depends on $\phi$ and $\phi'$ and not $\zeta$. However the variational principle of I, §3.1 provides an explicit, and constructive, method for eliminating the dependence on $\phi$ and $\phi'$ in favour of $\zeta$:

$$\mathscr{K}(\zeta,\eta) = \min_{\rho\Phi-\rho'\Phi'=\zeta} K(\phi,\phi',\eta) \quad \text{(with } \eta \text{ fixed)}. \tag{2.8}$$

### 2.1. *The KH problem on Fourier space*

To obtain the reduced Hamiltonian system (2.7), a finite-dimensional version of the variational principle (2.8) will be implemented. Let

$$\left.\begin{aligned} \phi(x,y,t) &= \tfrac{1}{2}e_0(t) + \sum_{n=1}^{N} \mathrm{e}^{nky}(e_n(t)\cos nkx + f_n(t)\sin nkx), \\ \phi'(x,y,t) &= \tfrac{1}{2}e'_0(t) + \sum_{n=1}^{N} \mathrm{e}^{-nky}(e'_n(t)\cos nkx + f'_n(t)\sin nkx). \end{aligned}\right\} \tag{2.9}$$

The coefficients $c_0(t)$, $e_0(t)$, $e'_0(t)$ and the mean value of $\eta(x,t)$ are important for mean flow effects. The development throughout is for the case of infinite depth and therefore the mean of $\eta(x,t)$ is set to zero and $c_0(t)$, $e_0(t)$ and $e'_0(t)$ can be determined from the other Fourier coefficients. However, the analysis can be generalized to include the case where the mean-flow interactions are important, for example, when the upper and/or lower fluid layers are of finite extent.

On the finite-dimensional space of Fourier coefficients, the constraint (1.2) takes the vector form

$$\rho\boldsymbol{M}^{+}\boldsymbol{h} - \rho'\boldsymbol{M}^{-}\boldsymbol{h}' = \widehat{\boldsymbol{\zeta}}, \tag{2.10}$$

where

$$\widehat{\boldsymbol{\zeta}} = \begin{Bmatrix} C \\ D \end{Bmatrix}, \quad \boldsymbol{h} = \begin{Bmatrix} e \\ f \end{Bmatrix} \quad \text{and} \quad \boldsymbol{h}' = \begin{Bmatrix} e' \\ f' \end{Bmatrix} \tag{2.11}$$

are $2N$-dimensional vectors of Fourier coefficients. The matrices $\boldsymbol{M}^{\pm}$ are non-symmetric $2N \times 2N$ matrices with

$$\boldsymbol{M}^{\pm} = \begin{bmatrix} \boldsymbol{M}_1^{\pm} & \boldsymbol{M}_2^{\pm} \\ \boldsymbol{M}_3^{\pm} & \boldsymbol{M}_4^{\pm} \end{bmatrix} \tag{2.12}$$

where $\boldsymbol{M}_j^{\pm}$, $j = 1,\ldots,4$ are $N \times N$ matrices that depend on $A_j$ and $B_j$, $j = 1,\ldots,N$. Explicit expressions for the matrices $\boldsymbol{M}^{\pm}$ are given in Appendix A.

Define $\boldsymbol{\Gamma}^{\pm}$ to be the following $2N \times 2N$ symmetric matrices:

$$\boldsymbol{\Gamma}^{\pm} = \begin{bmatrix} \boldsymbol{C}^{\pm} & -\boldsymbol{S}^{\pm} \\ \boldsymbol{S}^{\pm} & \boldsymbol{C}^{\pm} \end{bmatrix} \tag{2.13}$$

where $\boldsymbol{C}^{\pm}$ are $N \times N$ symmetric matrices and $\boldsymbol{S}^{\pm}$ are $N \times N$ skew-symmetric matrices. Explicit expressions for $\boldsymbol{\Gamma}^{\pm}$ are given in Appendix A. The matrices $\boldsymbol{\Gamma}^{\pm}$ are used to express the kinetic energy in matrix form. Substituting (2.5) and (2.9) into $K_1$ in equation (2.3) and using (2.13) results in

$$K_1 = \tfrac{1}{2}\rho\boldsymbol{h}^T\boldsymbol{\Gamma}^{+}\boldsymbol{h} + \tfrac{1}{2}\rho'\boldsymbol{h}'^T\boldsymbol{\Gamma}^{-}\boldsymbol{h}'. \tag{2.14}$$

For $K_2$ further notation is needed. Let $A' \in \mathbb{R}^N$ have entries $A'_n = nkA_n$ $(n = 1,\ldots,N)$

and $\boldsymbol{B}' \in \mathbb{R}^N$ have entries $B'_n = nkB_n$ $(n = 1, \ldots, N)$. Define the $2N$-vector

$$\boldsymbol{R}' = \begin{Bmatrix} \boldsymbol{A}' \\ \boldsymbol{B}' \end{Bmatrix} \tag{2.15}$$

and the $2N \times 2N$ unit symplectic matrix,

$$\boldsymbol{J} = \begin{bmatrix} 0 & \boldsymbol{I}_N \\ -\boldsymbol{I}_N & 0 \end{bmatrix}. \tag{2.16}$$

Then $K_2$ in (2.3) becomes

$$K_2 = \rho U \boldsymbol{R}'^T \boldsymbol{J} \boldsymbol{M}^+ \boldsymbol{h} - \rho' U' \boldsymbol{R}'^T \boldsymbol{J}\, \boldsymbol{M}^- \boldsymbol{h}' \tag{2.17}$$

where $\boldsymbol{M}^\pm$ are the matrices (2.12) that also appear in the definition of the constraint (2.10). The variational principle (2.8) is now the straightforward finite-dimensional constrained variational problem

$$\mathscr{K}(\boldsymbol{X}) = \min K(\boldsymbol{h}, \boldsymbol{h}'; \boldsymbol{A}, \boldsymbol{B}) \text{ for fixed } (\boldsymbol{A}, \boldsymbol{B}) \text{ subject to the constraint (2.10).}$$

This minimization problem can be carried out by introducing $\lambda \in \mathbb{R}^{2N}$ as a vector of Lagrange multipliers. Then a necessary condition for $(\boldsymbol{h}, \boldsymbol{h}')$ to minimize $K$ is that the Lagrange functional

$$\mathscr{L} = K_1(\boldsymbol{h}, \boldsymbol{h}') + K_2(\boldsymbol{h}, \boldsymbol{h}') - \boldsymbol{\lambda}^T \left\{ \rho \boldsymbol{M}^+ \boldsymbol{h} - \rho' \boldsymbol{M}^- \boldsymbol{h}' - \widehat{\boldsymbol{\zeta}} \right\}$$

should be stationary with respect to variations of $\boldsymbol{h}$ and $\boldsymbol{h}'$. The variations

$$\frac{\delta \mathscr{L}}{\delta \boldsymbol{h}} = \frac{\delta \mathscr{L}}{\delta \boldsymbol{h}'} = 0,$$

result in the following linear equations:

$$\left.\begin{aligned} \boldsymbol{\Gamma}^+ \boldsymbol{h} &= U \boldsymbol{M}^{+T} \boldsymbol{J} \boldsymbol{R}' + \boldsymbol{M}^{+T} \boldsymbol{\lambda}, \\ \boldsymbol{\Gamma}^- \boldsymbol{h}' &= -U' \boldsymbol{M}^{-T} \boldsymbol{J} \boldsymbol{R}' - \boldsymbol{M}^{-T} \boldsymbol{\lambda}. \end{aligned}\right\} \tag{2.18}$$

The matrices $\boldsymbol{\Gamma}^\pm$ are invertible (they are a perturbation of a diagonal matrix (see Appendix A)); therefore $\boldsymbol{h}$ and $\boldsymbol{h}'$ can be expressed as functions of $A_j$, $B_j$ $(j = 1, \ldots, N)$ and $\boldsymbol{\lambda}$. The vector of Lagrange multipliers is eliminated by substituting (2.22) into the constraint set (2.10). Introduce the matrices

$$\boldsymbol{P} = \rho \boldsymbol{P}^+ + \rho' \boldsymbol{P}^- \quad \text{where} \quad \boldsymbol{P}^\pm = \boldsymbol{M}^\pm \boldsymbol{\Gamma}^{\pm -1} \boldsymbol{M}^{\pm T}, \tag{2.19}$$

which are $2N \times 2N$ and symmetric. Substituting (2.18) into the constraint (2.10) and using (2.19) results in the following expression for the vector of Lagrange multipliers:

$$\boldsymbol{P} \boldsymbol{\lambda} = \widehat{\boldsymbol{\zeta}} - [\rho U \boldsymbol{P}^+ + \rho' U' \boldsymbol{P}^-] \boldsymbol{J} \boldsymbol{R}'. \tag{2.20}$$

Let

$$\widehat{\boldsymbol{\eta}} = \begin{Bmatrix} \boldsymbol{A} \\ \boldsymbol{B} \end{Bmatrix} \in \mathbb{R}^{2N} \tag{2.21}$$

represent the vector of Fourier coefficients for the wave height. In (2.20) the $2N$-vector of Lagrange multipliers is a function of $\widehat{\boldsymbol{\eta}}$ and $\widehat{\boldsymbol{\zeta}}$ only. Therefore substitution of (2.20) into the kinetic energy results in the unique solution of the minimization problem. After some algebra we obtain

$$\begin{aligned}\mathscr{K} &= \tfrac{1}{2}\widehat{\boldsymbol{\zeta}}^T \boldsymbol{P}^{-1}\widehat{\boldsymbol{\zeta}} - c_0 \widehat{\boldsymbol{\zeta}}^T \boldsymbol{J}\boldsymbol{R}' \\ &\quad + \frac{\rho\rho'}{\rho+\rho'}(U-U')\widehat{\boldsymbol{\zeta}}^T \boldsymbol{P}^{-1}[\boldsymbol{P}^+ - \boldsymbol{P}^-]\boldsymbol{J}\boldsymbol{R}' \\ &\quad + \tfrac{1}{2}\rho\rho'(U-U')^2 \boldsymbol{R}'^T \boldsymbol{J}\boldsymbol{P}^+\boldsymbol{P}^{-1}\boldsymbol{P}^-\boldsymbol{J}\boldsymbol{R}' \end{aligned} \tag{2.22}$$

where $c_0$ is defined in (1.15).

Let $\widehat{\boldsymbol{X}} = (\hat{\boldsymbol{\eta}}, \hat{\boldsymbol{\zeta}})^T \in \mathbb{R}^{4N}$, then it is clear that $\mathscr{K}$ is a function of the vector $\widehat{\boldsymbol{X}}$ of Fourier coefficients. The vector $\widehat{\boldsymbol{X}}$ is related to the vector $\boldsymbol{X}$ (cf. equation (2.6)) by a permutation matrix, say $\widehat{\boldsymbol{X}} = \boldsymbol{Q}X$ (an explicit expression for $\boldsymbol{Q}$ is easily written down but is not needed). Therefore the total energy – Hamiltonian function – takes the form

$$H(\boldsymbol{X}) = \mathscr{K}(\boldsymbol{X}) + \mathscr{V}(\boldsymbol{X}), \qquad \boldsymbol{X} \in \mathbb{R}^{4N} \tag{2.23}$$

for arbitrary but finite $N$, with $\mathscr{K}$ given in (2.22) and $\mathscr{V}(\boldsymbol{X})$ obtained by substituting the first equation of (2.5) into (2.2).

To obtain the symplectic form for the reduced system, $\Omega_N$, substitute (2.5) into $\Omega$ in (2.4), resulting in

$$\begin{aligned}\Omega_N &= \frac{2}{\ell}\int_0^\ell \left(\tfrac{1}{2}\mathrm{d}C_0\right) \wedge \left(\sum_{n=1}^N \mathrm{d}A_n \cos nkx + \mathrm{d}B_n \sin nkx\right) \mathrm{d}x \\ &\quad + \frac{2}{\ell}\int_0^\ell \left(\sum_{n=1}^N \mathrm{d}C_n \cos nkx + \mathrm{d}D_n \sin nkx\right) \wedge \left(\sum_{n=1}^N \mathrm{d}A_n \cos nkx + \mathrm{d}B_n \sin nkx\right) \mathrm{d}x \\ &= \sum_{n=1}^N (\mathrm{d}C_n \wedge \mathrm{d}A_n + \mathrm{d}D_n \wedge \mathrm{d}B_n)\end{aligned}$$

or in terms of a skew-symmetric bilinear form

$$\Omega_N(\boldsymbol{Y}_1, \boldsymbol{Y}_2) = -\langle \boldsymbol{J}_N \boldsymbol{Y}_1, \boldsymbol{Y}_2 \rangle$$

where $\boldsymbol{Y}_1$ and $\boldsymbol{Y}_2$ are arbitrary vectors in $\mathbb{R}^{4N}$, $\langle \cdot, \cdot \rangle$ is the standard inner product on $\mathbb{R}^{4N}$ and

$$\boldsymbol{J}_N = \mathrm{diag}(\underbrace{\boldsymbol{J}_2, \ldots, \boldsymbol{J}_2}_{N \text{ times}}) \quad \text{with} \quad \boldsymbol{J}_2 = \begin{pmatrix} \boldsymbol{0} & \boldsymbol{I}_2 \\ -\boldsymbol{I}_2 & \boldsymbol{0} \end{pmatrix}. \tag{2.24}$$

This completes the reduction of the KH problem on spatially periodic functions to the Hamiltonian system (2.7) on $\mathbb{R}^{4N}$ with $N$ arbitrary but finite.

### 2.2. *Critical points of the energy and TWs*

The translation invariance in $x$ of the equations and the Hamiltonian structure together lead to a natural variational principle for periodic TWs (cf. Benjamin 1984; I, §3.3).

The translation symmetry of the full KH problem will result in an $SO(2)$ symmetry on Fourier space. A representation for this group on the finite-dimensional space of Fourier coefficients is obtained as follows. The action of the translation group on functions is

$$\boldsymbol{T}_\theta \cdot \eta(x) = \eta(x+\theta) \quad \forall \theta \in \mathbb{R}. \tag{2.25}$$

To obtain the action of $\boldsymbol{T}_\theta$ on the space of Fourier coefficients, act on $\eta(x,t)$ in the

first expression in (2.5) with $\boldsymbol{T}_\theta$ to obtain,

$$\begin{aligned}\boldsymbol{T}_\theta \cdot \eta(x,t) = \eta(x+\theta,t) &= \sum_{n=1}^{N} A_n \cos nk(x+\theta) + B_n \sin nk(x+\theta) \\ &= \sum_{n=1}^{N} (A_n \cos nk\theta + B_n \sin nk\theta)\cos nkx \\ &\quad + \sum_{n=1}^{N} (-A_n \sin nk\theta + B_n \cos nk\theta)\sin nkx\,. \end{aligned} \tag{2.26}$$

Therefore on Fourier space, with coordinates $\boldsymbol{X} \in \mathbb{R}^{4N}$ (cf. equation (2.6)),

$$\boldsymbol{T}_\theta \cdot \boldsymbol{X} = (\boldsymbol{T}_{1\theta} \cdot \boldsymbol{X}_1, \ldots, \boldsymbol{T}_{n\theta} \cdot \boldsymbol{X}_n, \ldots, \boldsymbol{T}_{N\theta} \cdot \boldsymbol{X}_N) \tag{2.27}$$

with

$$\boldsymbol{T}_{n\theta} \cdot \boldsymbol{X}_n \stackrel{\text{def}}{=} \begin{bmatrix} \cos nk\theta & \sin nk\theta & 0 & 0 \\ -\sin nk\theta & \cos nk\theta & 0 & 0 \\ 0 & 0 & \cos nk\theta & \sin nk\theta \\ 0 & 0 & -\sin nk\theta & \cos nk\theta \end{bmatrix} \begin{pmatrix} A_n \\ B_n \\ C_n \\ D_n \end{pmatrix}.$$

On Fourier space, the translation invariance results in an action which is the direct sum of irreducible representations of the group $SO(2)$. The $SO(2)$-invariance of the Hamiltonian system (2.7) implies

$$H(\boldsymbol{T}_\theta \boldsymbol{X}) = H(\boldsymbol{X}) \quad \text{and} \quad \boldsymbol{T}_\theta^T \boldsymbol{J}_N \boldsymbol{T}_\theta = \boldsymbol{J}_N \quad \forall \theta \in SO(2)\,. \tag{2.28}$$

The connection between symmetry and conservation laws (I, §3.4) will also have a finite-dimensional counterpart. The impulse is given by

$$I = -\frac{2}{\ell}\int_0^\ell \zeta \eta_x \,\mathrm{d}x = \sum_{n=1}^{N} nk(A_n D_n - B_n C_n)\,.$$

In vector notation the impulse on Fourier space can be written in the two equivalent forms

$$I(\widehat{\boldsymbol{X}}) = -\widehat{\boldsymbol{\zeta}}^T \boldsymbol{J}\boldsymbol{R}' \quad \text{or} \quad I(\boldsymbol{X}) = \tfrac{1}{2}\langle \boldsymbol{X}, \boldsymbol{K}\boldsymbol{X}\rangle \tag{2.29}$$

where

$$\boldsymbol{K} = \mathrm{diag}(\boldsymbol{K}_1, \ldots, \boldsymbol{K}_N) \quad \text{with} \quad \boldsymbol{K}_n = nk \begin{pmatrix} 0 & 0 & 0 & 1 \\ 0 & 0 & -1 & 0 \\ 0 & -1 & 0 & 0 \\ 1 & 0 & 0 & 0 \end{pmatrix}.$$

Since $\nabla I(\boldsymbol{X}) = \boldsymbol{K}\boldsymbol{X}$, a short calculation, using (2.27), verifies that

$$\boldsymbol{J}_N \nabla I(\boldsymbol{X}) = \boldsymbol{J}_N \boldsymbol{K}\boldsymbol{X} = -\frac{\mathrm{d}}{\mathrm{d}\theta}\boldsymbol{T}_\theta \boldsymbol{X}\Big|_{\theta=0} \tag{2.30}$$

which is the finite-dimensional counterpart to I, equation (3.12). Note that the $SO(2)$ invariance of $H$ and (2.30) combine to prove that $I(X)$ is an invariant since

$$\begin{aligned} 0 = \frac{\mathrm{d}}{\mathrm{d}\theta} H(\boldsymbol{T}_\theta X)\Big|_{\theta=0} &= \left\langle \nabla H(\boldsymbol{X}), \frac{\mathrm{d}}{\mathrm{d}\theta}\boldsymbol{T}_\theta \boldsymbol{X}\Big|_{\theta=0} \right\rangle \\ &= -\left\langle \boldsymbol{J}_N \boldsymbol{X}_t, \frac{\mathrm{d}}{\mathrm{d}\theta}\boldsymbol{T}_\theta \boldsymbol{X}\Big|_{\theta=0} \right\rangle \quad (\boldsymbol{X}_t = \boldsymbol{J}_N \nabla H(\boldsymbol{X})) \end{aligned}$$

$$= \left\langle \boldsymbol{X}_t, \boldsymbol{J}_N \frac{\mathrm{d}}{\mathrm{d}\theta} \boldsymbol{T}_\theta \boldsymbol{X} \Big|_{\theta=0} \right\rangle \quad \text{(skew-symmetry of } \boldsymbol{J}_N\text{)}$$
$$= \langle \boldsymbol{X}_t, \nabla I(\boldsymbol{X}) \rangle \quad \text{(equation (2.30))}$$
$$= I_t \,.$$

The advantage of this variational structure is that periodic TWs are relative equilibria and given explicitly by

$$\boldsymbol{X}(t) = \boldsymbol{T}_{\theta(t)} \mathscr{U} \quad \text{with} \quad \theta(t) = -ct + \theta_0 \tag{2.31}$$

for some constant vector $\mathscr{U} \in \mathbb{R}^{4N}$, from which it follows that

$$\boldsymbol{X}_t = \frac{\mathrm{d}}{\mathrm{d}t} \boldsymbol{T}_{\theta(t)} \mathscr{U} = -c \boldsymbol{T}_{\theta(t)} \frac{\mathrm{d}}{\mathrm{d}\theta} \boldsymbol{T}_\theta \Big|_{\theta=0} \mathscr{U} = c \boldsymbol{T}_{\theta(t)} \boldsymbol{J}_N \nabla I(\mathscr{U}) \quad \text{(using (2.30))}\,.$$

Therefore, substituting (2.31) into (2.7) and using the $T_\theta$ invariance of $H$ results in

$$c \boldsymbol{T}_{\theta(t)} \boldsymbol{J}_N \nabla I(\mathscr{U}) = \boldsymbol{J}_N \nabla H(T_{\theta(t)} \mathscr{U}) = \boldsymbol{J}_N \boldsymbol{T}_{\theta(t)} \nabla H(\mathscr{U}) = \boldsymbol{T}_{\theta(t)} \boldsymbol{J}_N \nabla H(\mathscr{U})$$

or, since $T_{\theta(t)} \boldsymbol{J}_N$ is invertible,

$$\nabla H(\mathscr{U}) = c \nabla I(\mathscr{U})\,,$$

which defines the vector $\mathscr{U}$ in (2.31) and is the Lagrange necessary condition for the constrained variational principle: TWs correspond to relative equilibria of the form (2.31) with $\mathscr{U}$ a critical point of the energy on level sets of the impulse; a finite-dimensional version of I, §3.3, equation (3.14). Comparing (2.31) with (2.25) shows that (2.31) is a finite-dimensional version of a TW: $\eta(x,t) = \boldsymbol{T}_{\theta(t)} \eta(x) = \eta(x - ct + \theta_0)$.

Let

$$\mathscr{F}(\mathscr{U}, c) = H(\mathscr{U}) - cI(\mathscr{U}), \qquad \mathscr{U} \in \mathbb{R}^{4N}\,.$$

The $4N$-vector of Fourier coefficients satisfying $\nabla \mathscr{F} = 0$ is obtained by solving the $4N$ nonlinear equations

$$\frac{\partial \mathscr{F}}{\partial A_n} = \frac{\partial \mathscr{F}}{\partial B_n} = \frac{\partial \mathscr{F}}{\partial C_n} = \frac{\partial \mathscr{F}}{\partial D_n} = 0 \quad \text{for } n = 1, \ldots, N\,. \tag{2.32}$$

In the remainder of this section the $4N$ algebraic equations (2.32) are solved for $\|\mathscr{U}\|$ small and $N = 3$. First we obtain some general simplifications that are independent of $N$ but require $\|\mathscr{U}\|$ small.

The first step in the elimination is to solve for the vector $\widehat{\boldsymbol{\zeta}}$ in terms of $\widehat{\boldsymbol{\eta}}$. The equation $\delta \mathscr{F} / \delta \widehat{\boldsymbol{\zeta}} = 0$ must be solved where, by (2.22) and (2.29),

$$\begin{aligned} \mathscr{F}(\widehat{\boldsymbol{\zeta}}, \widehat{\boldsymbol{\eta}}; c) = V(\widehat{\boldsymbol{\eta}}) &+ \tfrac{1}{2} \widehat{\boldsymbol{\zeta}}^T \boldsymbol{P}^{-1} \widehat{\boldsymbol{\zeta}} + (c - c_0) \widehat{\boldsymbol{\zeta}}^T \boldsymbol{J} \boldsymbol{R}' \\ &+ \frac{\rho \rho'}{\rho + \rho'} (U - U') \widehat{\boldsymbol{\zeta}}^T \boldsymbol{P}^{-1} [\boldsymbol{P}^+ - \boldsymbol{P}^-] \boldsymbol{J} \boldsymbol{R}' \\ &+ \tfrac{1}{2} \rho \rho' (U - U')^2 \boldsymbol{R}'^T \boldsymbol{J} \boldsymbol{P}^+ \boldsymbol{P}^{-1} \boldsymbol{P}^- \boldsymbol{J} \boldsymbol{R}'\,. \end{aligned} \tag{2.33}$$

The variation of $\mathscr{F}$ with respect to $\widehat{\boldsymbol{\zeta}}$, with $\widehat{\boldsymbol{\eta}}$ fixed, results in a *linear* equation for $\widehat{\boldsymbol{\zeta}}$ which after some algebraic manipulation becomes

$$\widehat{\boldsymbol{\zeta}} = -(c - c_o) \boldsymbol{P} \boldsymbol{J} \boldsymbol{R}' - \frac{\rho \rho'}{\rho + \rho'} (U - U') [\boldsymbol{P}^+ - \boldsymbol{P}^-] \boldsymbol{J} \boldsymbol{R}'\,, \tag{2.34}$$

where $c_o = (\rho U + \rho' U')/(\rho + \rho')$ (cf. equation (1.15)). Explicit expressions for the

matrices $\boldsymbol{P}^{\pm}$ are given in Appendix A for $N = 3$. Back substitution of (2.34) into $\mathscr{F}$ in (2.33) reduces $\mathscr{F}$ to a function of $\hat{\boldsymbol{\eta}}$. After some algebra we obtain

$$\begin{aligned}\mathscr{F}(\hat{\boldsymbol{\zeta}}(\hat{\boldsymbol{\eta}};c),\hat{\boldsymbol{\eta}};c) = V(\hat{\boldsymbol{\eta}}) &+ \tfrac{1}{2}(c-c_0)^2\boldsymbol{R}'^{T}\boldsymbol{J}\boldsymbol{P}\boldsymbol{J}\boldsymbol{R}' \\ &+ \frac{\rho\rho'}{\rho+\rho'}(U-U')(c-c_0)\boldsymbol{R}'^{T}\boldsymbol{J}[\boldsymbol{P}^{+}-\boldsymbol{P}^{-}]\boldsymbol{J}\boldsymbol{R}' \\ &+ \tfrac{1}{2}\frac{\rho\rho'}{(\rho+\rho')^2}(U-U')^2\boldsymbol{R}'^{T}\boldsymbol{J}[\rho\boldsymbol{P}^{-}+\rho'\boldsymbol{P}^{+}]\boldsymbol{J}\boldsymbol{R}'. \end{aligned} \tag{2.35}$$

It remains to give an explicit expression for $V(\hat{\boldsymbol{\eta}})$. When $N = 3$ we find

$$\begin{aligned}V(\hat{\boldsymbol{\eta}}) = &\tfrac{1}{2}[(\rho-\rho')g+\sigma k^2](A_1^2+B_1^2) + \tfrac{1}{2}[(\rho-\rho')g+4\sigma k^2](A_2^2+B_2^2) \\ &+\tfrac{1}{2}[(\rho-\rho')g+9\sigma k^2](A_3^2+B_3^2) + \tfrac{5}{128}\sigma k^6(A_1^2+B_1^2)^3 \\ &-\tfrac{1}{8}\sigma k^4\left[\tfrac{3}{4}(A_1^2+B_1^2)^2 + 12(A_1^2+B_1^2)(A_2^2+B_2^2)\right] \\ &-\tfrac{3}{8}\sigma k^4\left[(B_3B_1^3 - A_3A_1^3) + 3A_1B_1(A_3B_1 - A_1B_3)\right] + \cdots. \end{aligned} \tag{2.36}$$

Using $\boldsymbol{P}^{\pm}$ in Appendix A and $V$ in (2.36) it is now straightforward to solve the four equations

$$\frac{\partial\mathscr{F}}{\partial A_3} = \frac{\partial\mathscr{F}}{\partial B_3} = \frac{\partial\mathscr{F}}{\partial A_2} = \frac{\partial\mathscr{F}}{\partial B_2} = 0 \tag{2.37}$$

to obtain $A_3$, $B_3$, $A_2$ and $B_2$ as functions of $A_1$ and $B_1$. Introduce the parameters

$$\chi = \frac{\rho\rho'}{\rho+\rho'}\frac{(U-U')^2}{k} \quad \text{and} \quad \beta_n = -(\rho-\rho')g + (\chi - n\sigma)nk^2, \qquad n = 1,2,\ldots. \tag{2.38}$$

Then, assuming $\beta_2\cdot\beta_3 \neq 0$, $\partial\mathscr{F}/\partial A_3 = \partial\mathscr{F}/\partial B_3 = 0$ results in

$$\left.\begin{aligned} A_3 &= \frac{k^4}{8\beta_3}(3\sigma-2\chi)A_1(A_1^2-3B_1^2) - \frac{2\chi rk^3}{\beta_3}(A_1A_2 - B_1B_2) + \cdots, \\ B_3 &= -\frac{k^4}{8\beta_3}(3\sigma-2\chi)B_1(B_1^2-3A_1^2) - \frac{2\chi rk^3}{\beta_3}(A_1B_2 + B_1A_2) + \cdots, \end{aligned}\right\} \tag{2.39}$$

and $\partial\mathscr{F}/\partial A_2 = \partial\mathscr{F}/\partial B_2 = 0$ results in

$$\begin{Bmatrix} A_2 \\ B_2 \end{Bmatrix} = \left[\gamma_1 + \gamma_2(A_1^2+B_1^2)\right]\begin{Bmatrix} A_1^2 - B_1^2 \\ 2A_1B_1 \end{Bmatrix} + \cdots \tag{2.40}$$

where

$$\gamma_1 = -\tfrac{1}{2}\frac{\chi rk^3}{\beta_2} + \frac{2}{\beta_2}\frac{\chi k^3}{(U-U')}(c-c_0), \tag{2.41}$$

$$\gamma_2 = \tfrac{3}{4}\frac{\chi rk^7}{\beta_2^2}(2\sigma-\chi) - \frac{2\chi^3r^3k^9}{\beta_3\beta_2^2} + \frac{1}{\beta_2}\left[\tfrac{7}{24}\chi rk^5 - \frac{\chi rk^7}{4\beta_3}(3\sigma-2\chi)\right]. \tag{2.42}$$

The conditions $\beta_n \neq 0$ for $n \geqslant 2$ are due to the presence of Wilton-type resonances. In particular when $\beta_2 = 0$ TW solutions with wavenumber $k$ and $2k$ simultaneously become unstable. The Wilton-type resonances near the KH instability are very interesting (cf. Nayfeh & Saric 1972, §5; Weissman 1979, Appendix B). Recent results on Wilton-type resonances for interfacial waves are given in Christodoulides & Dias (1994). The present analysis will be restricted to classes of TWs that occur away from such resonances.

Back substitution of (2.39)–(2.40) into $\mathscr{F}$ results in a reduced function depending

only on $A_1$, $B_1$, $c$ and parameters,

$$G(A_1, B_1; c) = \mathscr{F}(\widehat{\boldsymbol{\zeta}}(\widehat{\boldsymbol{\eta}}(A_1, B_1; c); c), \widehat{\boldsymbol{\eta}}(A_1, B_1; c); c)$$
$$= -\frac{1}{2k^2}(\beta_1 + k(\rho + \rho')(c - c_0)^2)z - \frac{1}{4k^2}v_1 z^2 - \frac{1}{6k^2}v_2 z^3 + \cdots, \quad (2.43)$$

where $z = k^2(A_1^2 + B_1^2)$,

$$v_1 = \tfrac{1}{2}k^2\left[\tfrac{3}{4}\sigma - \chi - \frac{\chi^2 r^2 k^2}{\beta_2} + \frac{8r\chi^2 k^2}{\beta_2(U - U')}(c - c_0)\right] \quad (2.44)$$

and

$$v_2 = \frac{k^2}{64}(22\chi - 15\sigma) + \frac{k^3}{64\beta_3}(3\sigma - 2\chi)[96r\chi\gamma_1 - 3k(3\sigma - 2\chi)]$$
$$+\tfrac{1}{4}\gamma_1^2\left[\frac{14}{k^2}\beta_2 - 18(\chi - 2\sigma) - 48\frac{\chi^2 r^2 k^2}{\beta_3}\right]. \quad (2.45)$$

The parameter $\gamma_1$ is defined in (2.41). The fact that $G(A_1, B_1; c)$ depends on the combination $A_1^2 + B_1^2$ only is due to the $SO(2)$-invariance of the functional $\mathscr{F}$.

The function $G$ is the reduced 'bifurcation function' for the TWs. Setting

$$g_1 = \frac{\partial G}{\partial A_1} = 0 \quad \text{and} \quad g_2 = \frac{\partial G}{\partial B_1} = 0 \quad (2.46)$$

results in a relation between the amplitude and the wave speed for travelling waves. However the nonlinear algebraic equations that result from (2.46) are quite complicated and contain some surprising results (cf. §2.3 and §2.5).

Before proceeding to the analysis of the critical points of $G$ it is shown that the equations (2.46), when suitably restricted, agree with previous results in the literature. Both Weissman (1979) and Miles (1986) obtain the coefficient $v_1$ using other methods and with suitable change of notation this expression agrees with theirs. The coefficient $v_2$ is new. However we can compare with previous results for special cases. When $\rho' = U = U' = 0$ and the amplitude is converted to the wave steepness, the expression for the velocity $c$ agrees with Hogan (1980, equation (3.7$g$)). Previous analytical results for interfacial waves carried to the fifth order are those of Tsuji & Nagata (1973) and Holyer (1979) who studied travelling waves at the interface between two quiescent fluids without surface tension. Setting $\sigma = U = U' = 0$ (resulting in $c_0 = 0$) and furthermore setting $B_1 = 0$ (wave height taken to be an even function), $\partial G/\partial A_1 = 0$ results in

$$c^2 = \frac{\rho - \rho'}{\rho + \rho'}\frac{g}{k}\left[1 + \frac{\rho^2 + \rho'^2}{(\rho + \rho')^2}k^2 A_1^2 + \frac{(\rho - \rho')^2}{4(\rho + \rho')^4}(5\rho^2 - 14\rho\rho' + 5\rho'^2)k^4 A_1^4\right],$$

which (with suitable changes of notation) agrees precisely with the result of Tsuji & Nagata (1973, p. 65, equation (19)). Furthermore with $B_1 = \sigma = U = U' = 0$ the coefficients $A_2$ and $A_3$ (obtained in (2.39) and (2.40)) for the wave height reduce to those obtained by Tsuji & Nagata (1973, p. 64, equation (15)).

### 2.3. *Generic bifurcation of TWs near the KH threshold*

TWs in the finite-dimensional Hamiltonian representation correspond to relative equilibria of the form $\boldsymbol{X}(t) = \boldsymbol{T}_{\theta(t)}\boldsymbol{\mathscr{U}}$ with $\boldsymbol{\mathscr{U}} \in \mathbb{R}^{4N}$ satisfying $\nabla H(\boldsymbol{\mathscr{U}}) = c\nabla I(\boldsymbol{\mathscr{U}})$. For $N = 3$, and $\|\boldsymbol{\mathscr{U}}\|$ sufficiently small, the solutions of this constrained critical point problem were shown to be in one-to-one correspondence with critical points of the

functional $G(A_1, B_1; c)$ in (2.43). In this subsection the critical points of $G$ for $v_1 \neq 0$ and their dependence on $c$, $u$ and $r$ are considered. Let

$$\boldsymbol{x} = (x_1, x_2) \stackrel{\text{def}}{=} (kA_1, kB_1), \quad z = x_1^2 + x_2^2 \quad \text{and} \quad \tau = \frac{(\rho - \rho')g}{\sigma k^2} \tag{2.47}$$

with the restriction $0 < \tau < 2$ ($\tau = 2$ corresponds to the Wilton-type 1 : 2 resonance). Then the bifurcation equation for periodic TWs is

$$\boldsymbol{g}(\boldsymbol{x}, c, u, r) \stackrel{\text{def}}{=} h(z, c, u, r) \begin{pmatrix} x_1 \\ x_2 \end{pmatrix} = -k \begin{pmatrix} \partial G/\partial A_1 \\ \partial G/\partial B_1 \end{pmatrix} = 0, \tag{2.48}$$

where

$$h(z, c, u, r) = D(c, u, r) + v_1 z + v_2 z^2 + \cdots \tag{2.49}$$

and

$$D(c, u, r) = \beta_1 + k(\rho + \rho')(c - c_0)^2,$$

with $v_1$ and $v_2$ defined in (2.44) and (2.45), and $\beta_1$ is defined in (2.38). The parameter $\tau$ does not appear explicitly in the parameter list. It is a ratio of gravitational forces to surface-tension forces and is important but will play a secondary role in the analysis. Non-trivial periodic TW solutions of small amplitude correspond to solutions of $h(z, c, u, r) = 0$.

The idea is to expand $h(z, c, u, r)$ in a Taylor series about the point $(z, c, u) = (0, c_0, u_0)$. A straightforward calculation using the definitions of $h$, $v_1$ and $v_2$ results in

$$\left.\begin{aligned} h^0 &= h(0, c_0, u_0, r) = D(c_0, u_0, r) = 0, \\ h_c^0 &= h_c(0, c_0, u_0, r) = \frac{\partial D}{\partial c}\bigg|_{(c_0, u_0, r)} = 0, \\ h_{cc}^0 &= h_{cc}(0, c_0, u_0, r) = \frac{\partial^2 D}{\partial c^2}\bigg|_{(c_0, u_0, r)} = 2k(\rho + \rho'), \end{aligned}\right\} \tag{2.50}$$

$$h_z^0 = h_z(0, c_0, u_0, r) = v_1(c_0, u_0, r) = \tfrac{1}{2}\sigma k^2 \frac{(\tau + 1)^2}{2 - \tau}(r^2 - r_0^2), \tag{2.51}$$

$$h_u^0 = h_u(0, c_0, u_0, r) = \frac{2}{u_0}(1 + \tau)\sigma k^2, \tag{2.52}$$

where $c_0$ and $u_0$ are defined in (1.15) and

$$r_0^2 = \frac{(4\tau + 1)(2 - \tau)}{4(\tau + 1)^2}.$$

Then, since $h^0 = h_c^0 = 0$, the leading terms in the Taylor expansion of $\boldsymbol{g}$ are

$$\boldsymbol{g} = \boldsymbol{x}[\tfrac{1}{2}h_{cc}^0(c - c_0)^2 + h_z^0 z + h_u^0(u - u_0) + \cdots]. \tag{2.53}$$

When $r \neq r_0$ it follows that $h_z^0 \neq 0$ and from (2.50) $h_{cc}^o > 0$, therefore introduce the scaling transformation

$$\widetilde{c} - \widetilde{c}_0 = (c - c_0)\left(\tfrac{1}{2}h_{cc}^0\right)^{1/2}, \quad \widetilde{z} = |h_z^0| z \quad \text{and} \quad \widetilde{u} - \widetilde{u}_0 = h_u^0(u - u_0).$$

Substitution into (2.53) and neglect of the higher-order terms in the Taylor expansion results in

$$\widetilde{\boldsymbol{x}}[(\widetilde{c} - \widetilde{c}_0)^2 + \epsilon\widetilde{z} + (\widetilde{u} - \widetilde{u}_0)] = 0 \tag{2.54}$$

where $\epsilon = \text{sign}(h_z^0)$. Equation (2.54) is the normalised truncated equation for the local

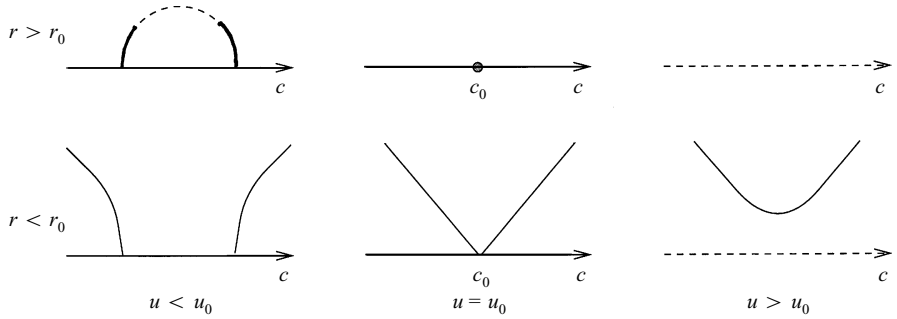


FIGURE 5. Branches of TWs in the amplitude–wave-speed plane near the KH instability when $r \neq r_0$. The dashed axis for $u > u_0$ corresponds to the KH unstable equilibrium and the dashed part of the branch for $r > r_0$ and $u < u_0$ corresponds to SH unstable TWs.

bifurcation of nonlinear periodic TWs near the KH instability (nearness measured by $|u - u_0|$). The KH threshold is $u = u_0$ and when $u > u_0$ the equilibrium solution (represented by $\boldsymbol{x} = 0$) is unstable.

The bifurcation diagrams for the TW solutions of (2.54) are shown in figure 5. The vertical direction in each diagram of figure 5 corresponds to scaled amplitude ($\tilde{z}^{1/2} \geqslant 0$). The two branches that join together when $r < r_0$ and $u = u_0$ detach from the origin and persist 'above' the unstable region. On the other hand when $r > r_0$ and $u < u_0$ the two families of TWs are *globally connected* and vanish into the origin when $u \geqslant u_0$ resulting in an absence of TW solutions when $u \geqslant u_0$ (at least locally). The SH instability that occurs along the branch for $r > r_0$ and $u < u_0$ will be verified in §3. The bifurcation of TWs for $r < r_0$ and $r > r_0$ is dramatically different. The singularity $r = r_0$ is considered in §2.5; it leads to quite complicated branching behaviour including bifurcation points and detached branches.

### 2.4. *Drazin's theory and time-modulation equations*

The critical features of the bifurcation of TWs and the SH instability for the case $r \neq r_0$ are already contained in the analysis of Drazin (1970). Using a Stuart–Watson expansion, Drazin derives a second-order ordinary differential equation for the complex amplitude $A(T)$ of a normal mode, as a model equation for the weakly nonlinear dynamics near the KH neutral curve, of the form

$$\frac{\mathrm{d}^2 A}{\mathrm{d}T^2} = -\alpha A + a|A|^2 A, \tag{2.55}$$

where $\mathrm{sign}(\alpha) = \mathrm{sign}(u_0 - u)$ and $\mathrm{sign}(a) = \mathrm{sign}(r - r_0)$ (cf. Drazin (1970, equation (41); Weissman 1979, §3). Drazin restricts $A$ to be real in (2.55) but a more complete picture is obtained by taking $A$ to be complex-valued.

In the model equation (2.55) TWs, of the full problem, are represented by

$$A(T) = A_0 \mathrm{e}^{\mathrm{i}\omega T} \quad \text{with} \quad \omega^2 + a|A_0|^2 = \alpha\,. \tag{2.56}$$

Taking into account that $\omega$ is shifted and scaled, (2.56) recovers exactly the results in equation (2.54) and figure 5.

Linearizing (2.55) about the state (2.56) results in

$$\frac{\mathrm{d}^2 B}{\mathrm{d}T^2} = -\alpha B + 2a|A_0|^2 B + A_0^2 \mathrm{e}^{2\mathrm{i}\omega T}\overline{B}\,,$$

which can be reduced to a constant-coefficient ODE by taking $B(T) = \mathrm{e}^{\mathrm{i}\omega T} C(T)$ with

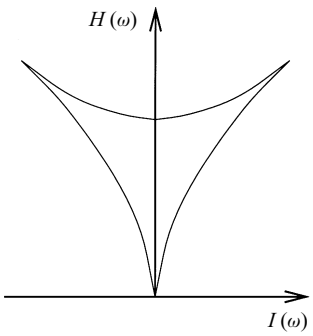


FIGURE 6. Evaluation of the functions $H(\omega)$ and $I(\omega)$, in equation (2.59) and below, along the branch of TWs (2.56) when $\alpha > 0$ and $a > 0$.

$C(T)$ satisfying

$$\frac{\mathrm{d}^2C}{\mathrm{d}T^2} + 2\mathrm{i}\omega\frac{\mathrm{d}C}{\mathrm{d}T} - a|A_0|^2C - aA_0^2\overline{C} = 0\,. \tag{2.57}$$

Taking $C(T) = C_1\mathrm{e}^{\lambda T} + C_2\mathrm{e}^{\bar{\lambda}T}$ the stability exponent $\lambda \in \mathbb{C}$ satisfies

$$\lambda^4 + 2(2\omega^2 - a|A_0|^2)\lambda^2 = 0\,. \tag{2.58}$$

When $a > 0$ and $\alpha > 0$ an instability – *a superharmonic instability* – occurs on the branch of TWs when $a|A_0|^2 > 2\omega^2$ (cf. figure 5). In other words, the model equation (2.55) predicts all the features of figure 5 including the SH instability. Although the model equation (2.55) and its prediction of SH instability predate the discovery of SH instability for water waves by several years, the precise nature of the instability predicted by (2.55) was not recognized at that time.

The model equation (2.55) is also a Hamiltonian system. Let

$$A = q_1 + \mathrm{i}q_2\,, \quad \frac{\mathrm{d}A}{\mathrm{d}T} = p_1 + \mathrm{i}p_2$$

and

$$H(q,p) = \tfrac{1}{2}(p_1^2 + p_2^2) + \tfrac{1}{2}\alpha(q_1^2 + q_2^2) - \tfrac{1}{4}a(q_1^2 + q_2^2)^2\,. \tag{2.59}$$

Then (2.55) is equivalent to

$$\dot{q}_j = \frac{\partial H}{\partial p_j}\,, \quad \dot{p}_j = -\frac{\partial H}{\partial q_j} \quad \text{for } j = 1,2$$

which is precisely the truncated normal form for the Hamiltonian Hopf bifurcation (cf. van der Meer 1985, p. 64). The above Hamiltonian system is integrable and the second integral is

$$I = p_2q_1 - p_1q_2 = \mathrm{Im}(\overline{A}A_T)\,.$$

A useful geometric picture is obtained by plotting the solution (2.56) in the $(H,I)$-plane. For example take $\alpha > 0$ and $a > 0$ and evaluate $H$ and $I$ on the branch of solutions (2.56),

$$H = \tfrac{1}{2}\omega^2|A_0|^2 + \tfrac{1}{2}\alpha|A_0|^2 - \tfrac{1}{4}a|A_0|^4 = \frac{1}{4a}(\alpha - \omega^2)(3\omega^2 + \alpha),$$
$$I = \omega|A_0|^2 = \frac{\omega}{a}(\alpha - \omega^2)\,.$$

Varying $\omega$ between $-\alpha^{1/2}$ and $\alpha^{1/2}$ results in a cut through a swallowtail with two

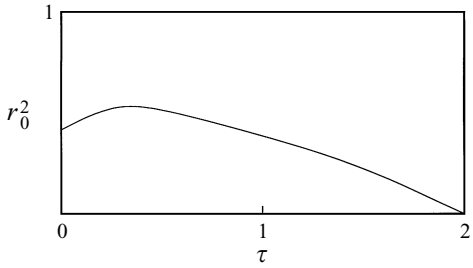


FIGURE 7. Critical value of the density ratio along the KH neutral curve.

cusp points as shown in figure 6 (compare with figure 4.19 of van der Meer 1985, p. 79). The cusp points correspond to the change from SH stable to SH unstable. In fact, in §3.3, this picture will be recovered for the full KH problem with $H$ and $I$ the energy and impulse for the KH problem (see Figure 15).

The model equation (2.55) breaks down if $a = 0$ (i.e. $r = r_0$) or $a$ is near zero. The KH problem near this degeneracy has never been considered. Weissman (1979, p. 653) suggests that when the coefficient $a$ is near zero the appropriate model equation is

$$\frac{\mathrm{d}^2A}{\mathrm{d}T^2} = -\alpha A + a|A|^2A + b|A|^4A$$

but this equation is incorrect. It is now well known that modulation equations with a small cubic term require more than the addition of a quintic term (cf. Johnson 1977; Eckhaus & Iooss 1989; Bridges 1994). One can infer from these results that the modulation equation (2.55) when $a$ is near zero has the form

$$\frac{\mathrm{d}^2A}{\mathrm{d}T^2} = -\alpha A - 2\mathrm{i}m|A|^2A_T + a|A|^2A + b|A|^4A$$

where the additional cubic term with coefficient $m \in \mathbb{R}$ is to be noted. Another argument in support of this form is that with $A(T) = A_0\mathrm{e}^{\mathrm{i}\omega T}$ the results to be presented in §2.5 are recovered (cf. equations (2.60) and (2.68)). However we will not consider this approach further, as, once the Hamiltonian framework for the bifurcation and SH instability are in place it is straightforward to consider the degenerate case in some completeness.

### 2.5. *Degenerate bifurcation ($r \approx r_0$) and multiple branching*

The singularity $r = r_o$ is associated with a distinguished value of the density ratio. The parameter $r_o$ depends on $\tau$ and the parameter $\tau$ can be thought of as parameterizing the KH neutral curve in the $(k, u)$-plane (see figure 2). The value $\tau = 2$ corresponds to $k = ((\rho - \rho')g/2\sigma)^{1/2}$ and at $\tau = 2$ a resonance occurs between waves of wavenumber $k$ and $2k$. The point $\tau = \tau_1 \approx 1.68$ will be defined shortly. Increasing $k$, and moving along the neutral curve, $\tau$ continuously decreases from $\tau = 2$ to $\tau = 0$ (as $k \to \infty$). The value $\tau = 1$ is associated with the minimum value of $u$ such that a KH instability occurs.

The distinguished point $r_0$ depends on $\tau$ and this dependence is plotted in figure 7. For example when $\tau = 1$, $r_0 = \frac{1}{4}\sqrt{5}$, therefore when $\tau = 1$, $r = r_0$ corresponds to

$$\frac{\rho'}{\rho} = \frac{4 - \sqrt{5}}{4 + \sqrt{5}} \approx 0.28$$

which is physically realistic. In other words, at any point along the neutral curve, with

$0 < \tau < 2$, a degeneracy ($r = r_0$) can be found at some physically realizable value of the density difference. Another reason for the interest in the singularity $r = r_o$ is that complicated bifurcations, that normally occur at large amplitude, arise at lower amplitudes due to the singularity and can therefore be studied analytically.

Recall the Taylor expansion of $g$ about the base point $(0, c_0, u_0)$,

$$\boldsymbol{g} = \left[\tfrac{1}{2}h^0_{cc}(c-c_0)^2 + h^0_z z + h^0_u(u-u_0) + \cdots\right]\boldsymbol{x}.$$

When $r = r_0$, $h^0_z = 0$ and therefore higher-order terms must be included to determine non-degenerate local branching behaviour. Expand $h_z$ about the point $r = r_0$ and the base point:

$$h_z = h^0_z + h^0_{zr}(r-r_0) + \tfrac{1}{2}h^0_{zz}z + h^0_{zc}(c-c_0) + \cdots.$$

Therefore when $h^0_z = 0$ a candidate local bifurcation equation is

$$\boldsymbol{g} = \left[\tfrac{1}{2}h^0_{cc}(c-c_0)^2 + h^0_{cz}(c-c_0)z + \tfrac{1}{2}h^0_{zz}z^2 + h^0_u(u-u_0) + h^0_{rz}(r-r_0)z + \cdots\right]\boldsymbol{x} = 0. \tag{2.60}$$

Here, we will truncate the higher-order terms and analyse the solution set. The solution set will correspond to the local bifurcation of TW branches in the neighbourhood of the singularity ($u = u_0$, $r = r_0$). The fact that the truncated Taylor expansion results in a non-degenerate function can be justified using $\mathbb{Z}_2$-equivariant singularity theory of Golubitsky & Schaeffer (1985, Chap. VI). An analysis along these lines has been carried out by Bridges (1990, 1991) for the general case of a finite-dimensional Hamiltonian systems with a collision of imaginary eigenvalues of opposite sign.

In (2.50) and (2.52) it was found that $h^0_{cc} > 0$ and $h^0_u > 0$. It remains to determine the derivatives $h^0_{zz}$, $h^0_{cz}$ and $h^0_{rz}$. Since $h = \beta_1 + v_1 z + v_2 z^2 + \cdots$ a straightforward calculation using the definitions for $v_1$ and $v_2$ in (2.44)–(2.45) results in

$$h^0_{zr} = \left.\frac{\partial v_1}{\partial r}\right|_{(c_0,u_0,r_0)} = \sigma k^2 r_0 \frac{(\tau+1)^2}{2-\tau} > 0, \tag{2.61}$$

$$h^0_{zc} = \left.\frac{\partial v_1}{\partial c}\right|_{(c_0,u_0,r_0)} = -4\sigma k^2 \frac{r_0}{u_0}\frac{(\tau+1)^2}{2-\tau} < 0, \tag{2.62}$$

$$h^0_{zz} = 2v_2(c_0,u_0,r_0) = \frac{\sigma k^2}{64(2-\tau)(3-\tau)}[30 + 67\tau + 326\tau^2 - 224\tau^3]. \tag{2.63}$$

In order for the truncated expression in (2.60) to be solvable it must be non-degenerate in some sense. First, it is necessary for all the Taylor coefficients to be non-zero and $h^0_{zr}$ and $h^0_{zc}$ are non-zero. Let

$$f(\tau) = 30 + 67\tau + 326\tau^2 - 224\tau^3,$$

then $h^0_{zz} \neq 0$ is equivalent to $f(\tau) \neq 0$ for $\tau \in (0,2)$. However $f(\tau_1) = 0$ where $\tau_1 \approx 1.68$ (the exact value is easily obtained but is not necessary here) and when $0 < \tau < \tau_1$, $f(\tau) > 0$ and for $\tau_1 < \tau < 2$, $f(\tau) < 0$ (see figure 2 for the location of $\tau_1$ on the KH neutral curve). Therefore define

$$\epsilon = \operatorname{sign}(h^0_{zz}) = \begin{cases} +1, & 0 < \tau < \tau_1, \\ -1, & \tau_1 < \tau < 2. \end{cases} \tag{2.64}$$

The singularity $\tau = \tau_1$ is not considered here. It is a singularity of codimension-3 and a complete analysis in the neighbourhood of $\tau = \tau_1$ would require retention of eighth-order terms in the reduced functional $G(A_1, B_1, c)$. Henceforth $\tau$ is restricted to $\tau \in (0,\tau_1) \cup (\tau_1, 2)$ in which case $h^0_{zz} \neq 0$.

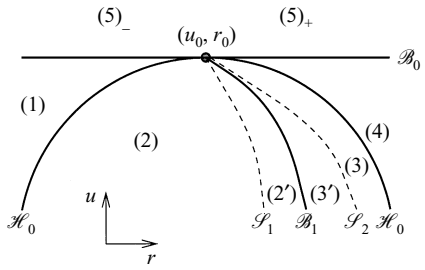


FIGURE 8. Components in the $(u,r)$-plane near $(u_0,r_0)$ with qualitatively distinct bifurcation diagrams for the case $0<\tau<\tau_1$ ($\epsilon=+1$).

The leading-order terms in (2.60) when $r=r_0$ and $u=u_0$ form a homogeneous quadratic in $(c-c_0)$ and $z$; that is,

$$h=\tfrac{1}{2}h^0_{cc}(c-c_0)^2+h^0_{cz}(c-c_0)z+\tfrac{1}{2}h^0_{zz}z^2+\cdots.$$

Therefore, in order for this expression to be non-degenerate we impose the additional condition that

$$\left(h^0_{zc}\right)^2-h^0_{cc}h^0_{zz}\neq 0 \tag{2.65}$$

which we will show is always satisfied. Let

$$m=\frac{h^0_{zc}}{(|h^0_{cc}h^0_{zz}|)^{1/2}}. \tag{2.66}$$

Then the condition in (2.65) is equivalent to $m^2\neq\epsilon$ (using the fact that $h^0_{cc}>0$) where $\epsilon$ is as defined in (2.64). Using the expressions for $h^0_{zc}$ and $h^0_{zz}$ in (2.62) and (2.63) we find that

$$m=-2\sqrt{2}\left[\frac{(8\tau^2+\tau+2)(3-\tau)(4\tau+1)}{(\tau+1)|f(\tau)|}\right]^{1/2} \tag{2.67}$$

and it is easy to show that $m<-1$ for all $\tau\in(0,2)$. Consequently $m^2>1$ and the non-degeneracy condition $m^2\neq\epsilon$ is never violated. Introduce the scaled variables

$$\widetilde{z}=z\left(\tfrac{1}{2}|h^0_{zz}|\right)^{1/2},\quad \widetilde{c}-\widetilde{c}_0=(c-c_0)\left(\tfrac{1}{2}h^0_{cc}\right)^{1/2},$$

$$\widetilde{u}-\widetilde{u}_0=h^0_u(u-u_0)\quad\text{and}\quad \widetilde{r}-\widetilde{r}_0=\frac{h^0_{rz}(r-r_0)}{\left(2|h^0_{zz}|\right)^{1/2}}.$$

Then $\boldsymbol{g}$ is transformed to (neglecting the higher-order terms)

$$\boldsymbol{g}=\boldsymbol{x}[(\widetilde{c}-\widetilde{c}_0)^2+2m(\widetilde{c}-\widetilde{c}_0)\widetilde{z}+\epsilon\widetilde{z}^2+(\widetilde{u}-\widetilde{u}_0)+2\widetilde{z}(\widetilde{r}-\widetilde{r}_0)]$$

where $m<-1$ according to (2.67) and $\epsilon=\pm1$. For simplicity drop the tildes in the scaled variables, then the normalized bifurcation equation for bifurcating TWs in the neighbourhood of $u=u_0$ and $r=r_0$ is

$$\boldsymbol{g}(\boldsymbol{x},c,u,r)=\boldsymbol{x}h(z,c,u,r) \tag{2.68}$$

with

$$h(z,c,u,r)=(c-c_0)^2+2m(c-c_0)z+\epsilon z^2+(u-u_0)+2z(r-r_0).$$

The bifurcation diagrams are obtained by setting $h=0$ for fixed $(u,r)$. There are qualitatively two sets of bifurcation diagrams, depending on whether $\epsilon=\pm1$.

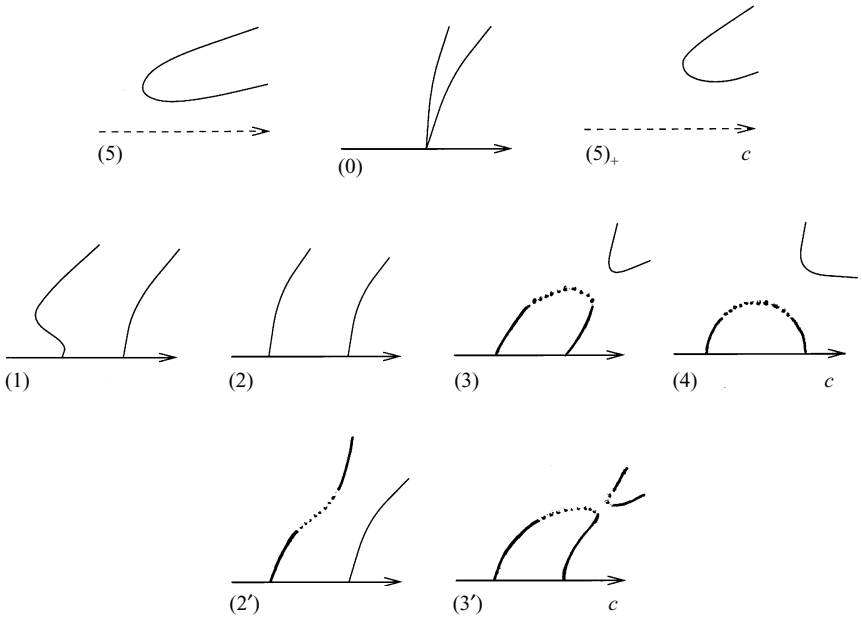


FIGURE 9. Branches of TWs in the amplitude–wave-speed plane corresponding to each of the components in figure 8 for $0 < \tau < \tau_1$ ($\epsilon = +1$). The label (0) corresponds to the point $(u_0, r_0)$.

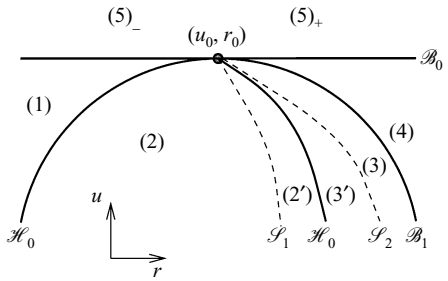


FIGURE 10. Components in the $(u,r)$-plane near $(u_0, r_0)$ with qualitatively distinct bifurcation diagrams for the case $\tau_1 < \tau < 2$ ($\epsilon = -1$).

The two-dimensional space $(u,r)$ will be composed of components each with a distinct branching diagram (cf. figures 8 and 10). The set of curves separating the components in figures 8 and 10 are defined as follows:

$$\begin{aligned}
\mathscr{B}_0 &\stackrel{\text{def}}{=} \{(u,r) \,:\, \exists\ c \text{ such that } h = h_c = 0 \text{ and } z = 0\} \\
&= \{(u,r) \,:\, u - u_0 = 0\}, \\
\mathscr{B}_1 &\stackrel{\text{def}}{=} \{(u,r) \,:\, \exists\ (c,z),\ z > 0 \text{ such that } h = h_z = h_c = 0\} \\
&= \{(u,r) \,:\, (r-r_0)^2 + (m^2 - \epsilon)(u - u_0) = 0,\ u \leqslant u_0,\ r \geqslant r_0\}, \\
\mathscr{H}_0 &\stackrel{\text{def}}{=} \{(u,r) \,:\, \exists\ c \text{ such that } h = h_z = 0 \text{ and } z = 0\} \\
&= \{(u,r) \,:\, (r-r_0)^2 + m^2(u - u_0) = 0,\ u \leqslant u_0\}\,.
\end{aligned}$$

Along the curves $\mathscr{B}_0$ and $\mathscr{B}_1$ a bifurcation occurs in the wave-speed–amplitude $(c, |\boldsymbol{x}|)$ plane and along the curve $\mathscr{H}_0$ a hysteresis point occurs in the $(c, |\boldsymbol{x}|)$ diagram. The curves $\mathscr{S}_1$ and $\mathscr{S}_2$ are associated with the SH instability and are defined in §3.4. To

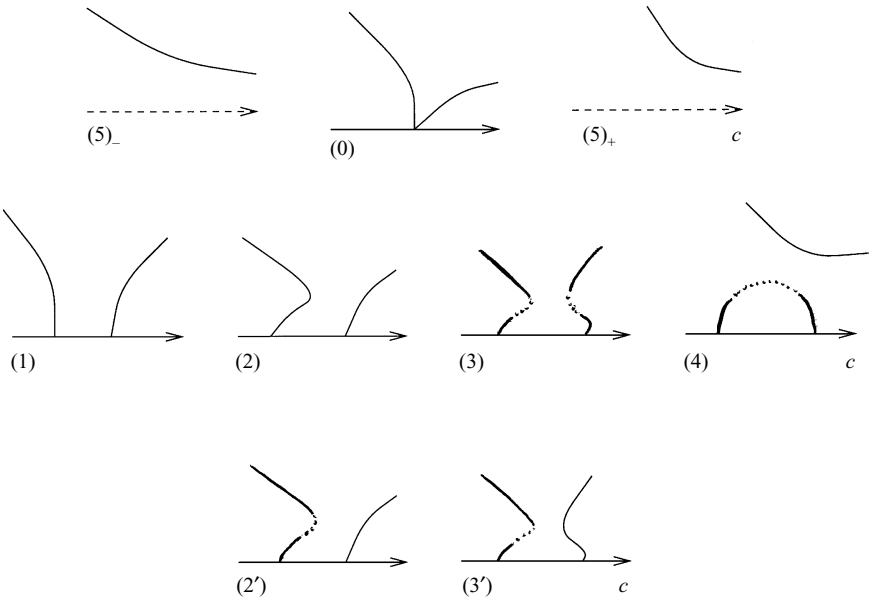


FIGURE 11. Branches of TWs in the amplitude–wave-speed plane corresponding to each of the components in figure 10 for $\tau_1 < \tau < 2$ ($\epsilon = -1$). The label (0) corresponds to the point $(u_0, r_o)$.

the left of the curve $\mathscr{S}_1$ in the $(u,r)$-plane all branches of TWs are SH stable. The bifurcation diagrams associated with figures 8 and 10 are shown in figures 9 and 11 respectively.

In the $(u,r)$-plane in figures 8 and 10 the region $u > u_0$ is the (KH) unstable region and is labelled $(5)_{\pm}$. Note that isolated branches of TWs persist in this region for both $r < r_0$ *and* $r > r_0$ (but $|r - r_0|$ small). The bifurcation diagrams for $u < u_0$ (diagrams (1), (2), (3) and (4)) show the breakup of the global loops. Note that the branching diagram in region (1) of figure 9 is identical to figure 5 (with $r < r_0$ and $u < u_0$) at *low amplitude*. However, at large amplitude (figure 9 region (1)) the left branch has a turning point and between regions (2) and (3) a bifurcation point moves in from infinity pinching off the global loop that must exist for $r \gg r_0$. In addition an isolated branch exists 'above' the global loop in region (4) and the isolated branch persists into the unstable region $(5)_+$. Although figure 5 showed the absence of TWs when $r > r_0$ and $u \geqslant u_0$, figures 9 and 11 show that in fact (at least for $|r - r_0|$ small) isolated branches of TWs do exist above the (KH) unstable equilibrium region when $r > r_0$. Using a numerical scheme, Robinet (1993) has confirmed many of the bifurcation pictures in figures 9 and 11. The dashed (solid) lines in figures 9 and 11 correspond to SH unstable (stable) TWs and these stability results are verified in §3.

## 3. Interaction between the SH instability and KH instability

The SH instability corresponds to a loss of stability of a TW to a class of perturbations of the same wavelength as the basic state. Moreover it corresponds to an eigenvalue of the linearized stability equation passing through the origin. The SH instability was first found in the numerical calculations of Longuet-Higgins (1978). Subsequently Tanaka (1983, 1985) discovered, in further numerical calculations, that the SH instability for water waves is associated with a maximum of the (disturbance)

energy, considered as a function of the wave speed. Saffman (1985) proved that when $\mathrm{d}H/\mathrm{d}c = 0$, where $H$ is the total (disturbance) energy and $c$ the wave speed, there is a quadruplet of eigenvalues of the time-dependent problem which accumulate at zero, with two due to symmetry, and the other two associated with a change of stability (cf. figure 13). The proof of Saffman used only the Hamiltonian structure; in particular, a finite-dimensional approximation for water waves based on the Zakharov formulation. Recent work on the SH instability has focused on the connection between SH instability and wave breaking (cf. Tanaka *et al.* 1987; Jillians 1989; Longuet-Higgins & Cleaver 1994). Jillians' numerical calculations indicate that all periodic SH unstable modes develop to wave breaking.

In this section, Saffman's theory for the SH instability is extended and applied to the bifurcating TWs near the KH unstable equilibrium. When $\mathrm{d}H/\mathrm{d}c \neq 0$, Saffman's theory does not indicate whether $\mathrm{d}H/\mathrm{d}c$ positive or negative is associated with stability. In other words, a change of stability occurring when $\mathrm{d}H/\mathrm{d}c = 0$ may correspond to either stability $\rightarrow$ instability or instability $\rightarrow$ stability.

However, with additional information, which is available within the Hamiltonian structure, we will show that the sign of $\mathrm{d}H/\mathrm{d}c$ associated with stability and instability can be determined. First we note that, since $\nabla H(\mathscr{U}) = c\nabla I(\mathscr{U})$ for a TW, it follows that $\mathrm{sign}(\mathrm{d}H/\mathrm{d}c) = \mathrm{sign}(\mathrm{d}I/\mathrm{d}c)$ when $c > 0$. Therefore without loss of generality we can analyse $\mathrm{d}I/\mathrm{d}c$. Let $\mathrm{L}(\mathscr{U}, c)$ be the linear operator associated with the second variation of $H(\mathscr{U}) - cI(\mathscr{U})$,

$$\mathrm{L}(\mathscr{U}, c) = D^2H(\mathscr{U}) - cD^2I(\mathscr{U}), \tag{3.1}$$

which, for the finite-dimensional Hamiltonian system (2.7), is a $4N \times 4N$ symmetric matrix. Let $\Pi$ be the product of the *non-zero* eigenvalues of $\mathrm{L}(\mathscr{U}, c)$. Then we will show that when $\Pi\,\mathrm{d}I/\mathrm{d}c < 0$ the TW is SH unstable. In fact, for the bifurcating TW near the KH instability, the spectrum of $\mathrm{L}(\mathscr{U}, c)$ can be explicitly analyzed. From the spectral information we will be able to show that the bifurcating TWs are SH stable (unstable) precisely when $\Pi\,\mathrm{d}I/\mathrm{d}c > 0$ (respectively $\Pi\,\mathrm{d}I/\mathrm{d}c < 0$). Using this theory we will be able to verify the SH instabilities that are shown in figures 5, 9 and 11.

### 3.1. *Impulse, wave speed and unstable eigenvalues*

The Hamiltonian system (2.7) is taken as a starting point, and it is assumed that there exists a one-parameter family of relative equilibria (TW) of the form (2.31) with $\nabla H(\mathscr{U}) = c\nabla I(\mathscr{U})$, denoted by $(\mathscr{U}(c), c)$. Define the tangent vector to the solution orbit by

$$\boldsymbol{g}(\mathscr{U}) = -\frac{\mathrm{d}}{\mathrm{d}\theta}\boldsymbol{T}_\theta\mathscr{U}\bigg|_{\theta=0}. \tag{3.2}$$

Then from (2.30) we have that

$$\boldsymbol{g}(\mathscr{U}) = \boldsymbol{J}_N\nabla I(\mathscr{U}). \tag{3.3}$$

Given a branch of relative equilibria the linear stability problem is formulated as follows. Linearizing (2.7) about $\boldsymbol{T}_{\theta(t)}\mathscr{U}$ results in

$$\widehat{\boldsymbol{Z}}_t = \boldsymbol{J}_N D^2H(\boldsymbol{T}_{\theta(t)}\mathscr{U})\widehat{\boldsymbol{Z}},$$

which has time-dependent coefficients. Therefore let $\widehat{\boldsymbol{Z}}(t) = \boldsymbol{T}_{\theta(t)}Z(t)$, with $\theta(t) = -ct + \theta_0$. Then, noting from the $SO(2)$-invariance of $H$, that $\boldsymbol{T}_\theta D^2H(\mathscr{U}) =$

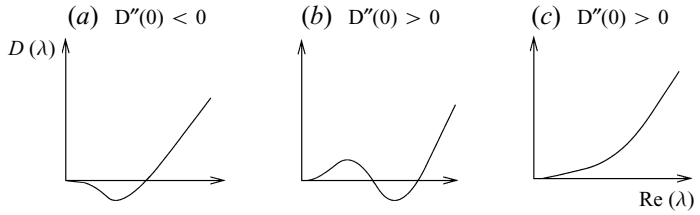


FIGURE 12. Possible behaviour of the spectral function D($\lambda$) along the Re($\lambda$) axis when (*a*) D″(0) < 0, (*b*) D″(0) > 0 and (*c*) D″(0) > 0.

$D^2H(\boldsymbol{T}_\theta\mathscr{U})\boldsymbol{T}_\theta$, the linear stability equation reduces to

$$\frac{\mathrm{d}}{\mathrm{d}t}(\boldsymbol{T}_{\theta(t)}Z(t)) = \boldsymbol{J}_N\boldsymbol{T}_{\theta(t)}D^2H(\mathscr{U})Z(t) = \boldsymbol{T}_{\theta(t)}\boldsymbol{J}_N D^2H(\mathscr{U})Z(t)$$

and so, after dividing out $\boldsymbol{T}_\theta$,

$$Z_t = \boldsymbol{J}_N D^2H(\mathscr{U})Z - c\boldsymbol{J}_N\nabla I(Z) = \boldsymbol{J}_N[D^2H(\mathscr{U}) - cD^2I(\mathscr{U})]Z = \boldsymbol{J}_N\mathrm{L}(\mathscr{U},c)Z \quad (3.4)$$

which has constant coefficients. The second equality in (3.4) follows since $\nabla I(Z) = \boldsymbol{K}Z = D^2I(\mathscr{U})Z$ (see equation (2.29)). Therefore $\lambda \in \mathbb{C}$ is a stability exponent of the linearised system (3.4) if D($\lambda$) = 0 where

$$\mathrm{D}(\lambda) = \det[\mathrm{L}(\mathscr{U},c) + \lambda\boldsymbol{J}_N]. \quad (3.5)$$

The linear operator L($\mathscr{U},c$) is defined in (3.1). The relative equilibrium (TW) $\boldsymbol{T}_{\theta(t)}\mathscr{U}$ is linearly unstable if there exists a $\lambda \in \mathbb{C}$ with Re($\lambda$) > 0 satisfying D($\lambda$) = 0. Note that D($\lambda$) is real when $\lambda$ is real.

Since $\det(\boldsymbol{J}_N) = 1$ and the dimension of the matrix $\boldsymbol{J}_N$ is even it follows that

$$\mathrm{D}(\lambda) = \lambda^{4N} + \text{terms of lower degree}$$

and so, when D($\lambda$) is restricted to the real axis, D($\lambda$) is positive for Re($\lambda$) sufficiently large.

D($\lambda$) is an even function of $\lambda$ since L($\mathscr{U},c$) is symmetric, $\boldsymbol{J}_N$ is skew-symmetric and the determinant is invariant under transposition:

$$\mathrm{D}(\lambda) = \det[\mathrm{L}(\mathscr{U},c) + \lambda\boldsymbol{J}_N] = \det[\mathrm{L}(\mathscr{U},c)^T + \lambda\boldsymbol{J}_N^T] = \det[\mathrm{L}(\mathscr{U},c) - \lambda\boldsymbol{J}_N] = \mathrm{D}(-\lambda).$$

Because of symmetry D(0) = 0. This can be seen as follows. Since $H(\boldsymbol{X})$ and $I(\boldsymbol{X})$ are $\boldsymbol{T}_\theta$-invariant it follows that

$$\nabla H(\boldsymbol{T}_\theta\mathscr{U}) - c\nabla I(\boldsymbol{T}_\theta\mathscr{U}) = 0 \quad \forall\theta \in SO(2)$$

and so defining $\xi_1 = \boldsymbol{g}(\mathscr{U})$

$$0 = \frac{\mathrm{d}}{\mathrm{d}\theta}[\nabla H(\boldsymbol{T}_\theta\mathscr{U}) - c\nabla I(\boldsymbol{T}_\theta\mathscr{U})]\bigg|_{\theta=0} = \mathrm{L}(\mathscr{U},c)\xi_1.$$

Since D(0) = $\det[\mathrm{L}(\mathscr{U},c)]$ and D($\lambda$) is even we have proved that

$$\mathrm{D}(0) = \mathrm{D}'(0) = 0.$$

Therefore D″(0) < 0 is a sufficient condition for instability; that is, since D($\lambda$) is positive for $\lambda \in \mathbb{R}$ with $\lambda$ sufficiently large, there is at least one value of $\lambda \in \mathbb{R}$ with $\lambda > 0$ such that D($\lambda$) = 0. A typical picture when D″(0) < 0 is shown in figure 12(*a*); although, under the stated conditions, it is also possible for D($\lambda$) to have more (but

an odd number of) real zeros. To connect the sign of $\mathrm{D}''(0)$ with $\mathrm{d}I/\mathrm{d}c$, the spectrum of $\mathrm{L}(\mathscr{U},c)$ and the identity (3.3) are used.

The matrix $\mathrm{L}(\mathscr{U},c)$ is symmetric and therefore its spectrum is real. Denote the eigenvalues of $\mathrm{L}(\mathscr{U},c)$ by $\mu_j$, $j=1,\dots,4N$ and the corresponding eigenvectors by $\xi_j$, $j=1,\dots,4N$,

$$\mathrm{L}(\mathscr{U},c)\boldsymbol{\xi}_j=\mu_j\boldsymbol{\xi}_j\,,\quad j=1,\dots,4N\,.$$

Owing to symmetry, $\mathrm{L}(\mathscr{U},c)\boldsymbol{\xi}_1=0$ and so $\mu_1=0$. Assuming $\mu_2,\dots,\mu_{4N}$ are non-zero, we will prove that

$$\mathrm{D}''(0)=2\,\Pi\,\frac{\mathrm{d}I}{\mathrm{d}c}\quad\text{where}\quad \Pi=\prod_{j=2}^{4N}\mu_j\,. \tag{3.6}$$

Let $\boldsymbol{\Sigma}$ be the $4N\times 4N$ matrix whose columns are the orthonormalized eigenvectors of $\mathrm{L}(\mathscr{U},c)$. Then

$$\boldsymbol{\Sigma}^T\mathrm{L}(\mathscr{U},c)\boldsymbol{\Sigma}=\boldsymbol{\Lambda}=\mathrm{diag}[0,\mu_2,\dots,\mu_{4N}]\,,$$

and

$$\mathrm{D}(\lambda)=\det[\mathrm{L}(\mathscr{U},c)+\lambda\boldsymbol{J}_N]=\det[\boldsymbol{\Sigma}^T(\mathrm{L}(\mathscr{U},c)+\lambda\boldsymbol{J}_N)\boldsymbol{\Sigma}]=\det[\boldsymbol{\Lambda}+\lambda\boldsymbol{K}]$$

where

$$\boldsymbol{K}=\boldsymbol{\Sigma}^T\boldsymbol{J}_N\boldsymbol{\Sigma}=\begin{bmatrix}0 & -\boldsymbol{a}^T\\ \boldsymbol{a} & \widehat{\boldsymbol{K}}\end{bmatrix}\,.$$

The particular form of $\widehat{\boldsymbol{K}}$, which is a $(4N-1)\times(4N-1)$ skew-symmetric matrix, is not important. However the vector $\mathbf{a}$ has an interesting characterization:

$$\boldsymbol{a}\in\mathbb{R}^{4N-1}\text{ with }\boldsymbol{a}_j=-\langle\boldsymbol{\xi}_1,\boldsymbol{J}_N\boldsymbol{\xi}_j\rangle\,,\ j=2,\dots,4N\,.$$

But $\boldsymbol{J}_N\boldsymbol{\xi}_1=\boldsymbol{J}_N\boldsymbol{g}(\mathscr{U})=-\nabla I(\mathscr{U})$ (using (3.3)) and so $\boldsymbol{a}_j$ are the coefficients of the eigenfunction expansion

$$-\nabla I(\mathscr{U})=\sum_{j=2}^{4N}\boldsymbol{a}_j\boldsymbol{\xi}_j\,. \tag{3.7}$$

Define $\widehat{\boldsymbol{\Lambda}}=\mathrm{diag}[\mu_2,\mu_3,\dots,\mu_{4N}]$ and suppose $\lambda$ is sufficiently small so that $\det[\widehat{\boldsymbol{\Lambda}}+\lambda\widehat{\boldsymbol{K}}]\neq 0$. Then

$$\begin{aligned}\mathrm{D}(\lambda)&=\det\left[\boldsymbol{\Lambda}+\lambda\begin{pmatrix}0 & -\boldsymbol{a}^T\\ \boldsymbol{a} & \widehat{\boldsymbol{K}}\end{pmatrix}\right]=\det\left[\begin{pmatrix}0 & -\lambda\boldsymbol{a}^T\\ +\lambda\boldsymbol{a} & \widehat{\boldsymbol{\Lambda}}+\lambda\widehat{\boldsymbol{K}}\end{pmatrix}\right]\\&=\det\left[\begin{pmatrix}0 & -\lambda\boldsymbol{a}^T\\ +\lambda\boldsymbol{a} & \widehat{\boldsymbol{\Lambda}}+\lambda\widehat{\boldsymbol{K}}\end{pmatrix}\begin{pmatrix}1 & \boldsymbol{0}^T\\ -\lambda[\widehat{\boldsymbol{\Lambda}}+\lambda\boldsymbol{K}]^{-1}\boldsymbol{a} & \boldsymbol{I}_{4N-1}\end{pmatrix}\right]\\&=\lambda^2\det[\widehat{\boldsymbol{\Lambda}}+\lambda\widehat{\boldsymbol{K}}]\boldsymbol{a}^T[\widehat{\boldsymbol{\Lambda}}+\lambda\widehat{\boldsymbol{K}}]^{-1}\boldsymbol{a}\end{aligned} \tag{3.8}$$

and so, since $\det\widehat{\boldsymbol{\Lambda}}=\Pi$,

$$\mathrm{D}''(0)=2\det[\widehat{\boldsymbol{\Lambda}}]\sum_{j=2}^{4N}\frac{1}{\mu_j}\boldsymbol{a}_j^2=2\,\Pi\sum_{j=2}^{4N}\frac{1}{\mu_j}\boldsymbol{a}_j^2\,. \tag{3.9}$$

Now, differentiating $\nabla H(\mathscr{U})=c\nabla I(\mathscr{U})$ with respect to $c$ results in

$$\mathrm{L}(\mathscr{U},c)\frac{\mathrm{d}\mathscr{U}}{\mathrm{d}c}=\nabla I(\mathscr{U})=-\sum_{j=2}^{4N}\boldsymbol{a}_j\boldsymbol{\xi}_j\,, \tag{3.10}$$

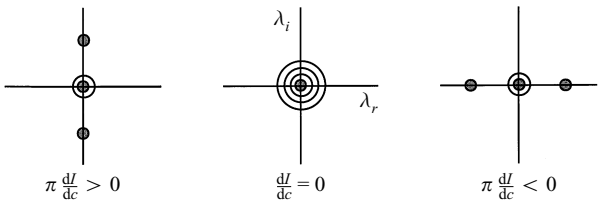


FIGURE 13. Position of the critical eigenvalues in the spectrum of the linearization in (3.4) near $I_c = 0$.

the second equality following from (3.7). Equation (3.10) is solvable using an eigenfunction expansion resulting in $\mathrm{d}\boldsymbol{\mathcal{U}}/\mathrm{d}c = -\sum_{j=2}^{4N} \boldsymbol{a}_j/\mu_j \boldsymbol{\xi}_j$, plus an arbitrary multiple of $\boldsymbol{\xi}_1$. Therefore

$$\frac{\mathrm{d}I}{\mathrm{d}c} = \langle \nabla I(\boldsymbol{\mathcal{U}}), \mathrm{d}\boldsymbol{\mathcal{U}}/\mathrm{d}c \rangle = \sum_{j=2}^{4N} \boldsymbol{a}_j^2/\mu_j \,,$$

which when substituted into (3.9) completes the proof of (3.6). Saffman's Theorem is implicit in (3.6) since $dH/dc = 0$ implies $\mathrm{d}I/\mathrm{d}c = 0$ (when $c \neq 0$) and $\mathrm{d}I/\mathrm{d}c = 0$ and the evenness of $\mathrm{D}(\lambda)$ imply that 0 is an eigenvalue of multiplicity four – assuming that $\mathrm{L}(\boldsymbol{\mathcal{U}}, c)$ has only one zero eigenvalue. But (3.6) also contains sufficient information to determine which sign of $\mathrm{d}I/\mathrm{d}c$ (or $\mathrm{d}H/\mathrm{d}c$) corresponds to instability.

$\mathrm{D}''(0) > 0$ is a necessary but not sufficient condition for SH stability. When $\mathrm{D}''(0) > 0$ the spectral function $\mathrm{D}(\lambda)$ could behave along the real axis as shown in either figure 12(*b*) or 12(*c*). It could also have roots with non-zero imaginary parts and $\mathrm{Re}(\lambda) > 0$. However, for the TW branches near the KH instability we will prove that when $\Pi\,\mathrm{d}I/\mathrm{d}c > 0$ the spectral function $\mathrm{D}(\lambda)$ has no roots in the complex half-plane $\mathrm{Re}(\lambda) > 0$, and hence the TW solutions are SH stable. When $\Pi\,\mathrm{d}I/\mathrm{d}c > 0$ for a TW, it is shown in Appendix B that it is a strict minimum of the energy on the constraint set of constant impulse and therefore the spectrum of $\boldsymbol{J}_N \mathrm{L}(\boldsymbol{\mathcal{U}}, c)$ is purely imaginary, with the only zero eigenvalue due to symmetry. The position of the critical eigenvalues in the spectrum of $\boldsymbol{J}_N \mathrm{L}(\boldsymbol{\mathcal{U}}, c)$, along a branch of TWs near a point where $\mathrm{d}I/\mathrm{d}c = 0$ is depicted in figure 13.

### 3.2. $\mathrm{L}(\boldsymbol{\mathcal{U}}, c)$ *near the KH instability*

In this subsection we show that the spectrum of $\mathrm{L}(\boldsymbol{\mathcal{U}}, c)$, evaluated at a TW near the KH point, has the following characterization:

$$\boldsymbol{\Sigma}(\mathrm{L}(\boldsymbol{\mathcal{U}}, c)) = \{0\} \cup \boldsymbol{\mu}_2 \cup \sigma_p \tag{3.11}$$

where $\sigma_p$ consists of $4N - 2$ positive eigenvalues. Moreover, it will be shown that

$$\mathrm{sign}(\mu_2) = -\mathrm{sign}(h_z) \tag{3.12}$$

where $h(z, c, u, r)$ is the reduced bifurcation function defined in equation (2.49). Based on (3.11), (3.12) and the theory for SH instability in §3.1 we define the following function whose sign will be in one-to-one correspondence with the SH stability ($\Delta_{SH} > 0$) and SH instability ($\Delta_{SH} < 0$):

$$\Delta_{SH}(z, c, u, r) = -h_z \frac{\mathrm{d}I}{\mathrm{d}c}, \quad \text{since } \mathrm{sign}(\Pi) = \mathrm{sign}(\mu_2)\,. \tag{3.13}$$

It follows immediately from the analysis in §3.1 that $\Delta_{SH} < 0$ corresponds to SH instability. The converse is a necessary but not sufficient condition for stability.

However we show in Appendix B that $\Delta_{SH} > 0$ corresponds to SH stability. The BF class of instabilities will be considered in §4.

The spectrum of $\mathrm{L}(\mathscr{U}, c)$ is composed of three parts as indicated in (3.11). The zero eigenvalue is due to symmetry. For the critical eigenvalue $\boldsymbol{\mu}_2$ the expression in (3.12), verified in Appendix C, is quite natural and is related to the Hessian of the reduced function $G(A_1, B_1; c)$, defined in (2.43), since

$$\left(\frac{\partial G}{\partial A_1}, \frac{\partial G}{\partial B_1}\right) = -2(A_1, B_1)\, h(z, c, u, r) = 0\,. \tag{3.14}$$

Therefore the Hessian of $G$ is

$$\mathrm{Hess}_{(A_1,B_1)}(G) = \begin{bmatrix} -2h - 4A_1^2 h_z & -4A_1 B_1\, h_z \\ -4A_1 B_1\, h_z & -2h - 4B_1^2 h_z \end{bmatrix}.$$

Along a solution branch $h = 0$ and it is clear that the determinant of $\mathrm{Hess}_{(A_1,B_1)}(G)$ evaluated at a solution is zero. Therefore the sign of the only non-zero eigenvalue of the Hessian of $G$ is

$$\mathrm{sign}(\mathrm{Tr}(\mathrm{Hess}_{(A_1,B_1)}(G))) = -\mathrm{sign}(h_z)\,.$$

(The minus sign arises due to the convention introduced in §2.3 when analyzing the bifurcation equation.)

It remains to verify that $\mathrm{L}(\mathscr{U}, c)$ has $4N-2$ positive eigenvalues. The argument is that if $\mathrm{L}(0, c_0)$ has $4N-2$ positive eigenvalues then, for $\|\mathscr{U}\|$ and $|c - c_0|$ sufficiently small, these eigenvalues will remain positive. When $\mathscr{U} = 0$ the matrix $\mathrm{L}(0, c_0)$ is *diagonal*. This follows from the expression for $\mathscr{F}$ in (2.33) by noting that the matrices $\boldsymbol{P}^{\pm}$ are diagonal when $\mathscr{U} = 0$. Let $\boldsymbol{L}_0$ represent $\mathrm{L}(0, c_0)$, then

$$\boldsymbol{L}_0 = \mathrm{diag}[\boldsymbol{L}_0^{(1)}, \ldots, \boldsymbol{L}_0^{(n)}, \ldots, \boldsymbol{L}_0^{(N)}], \tag{3.15}$$

where each of the matrices $\boldsymbol{L}_0^{(n)}$ are $4 \times 4$ diagonal matrices given by

$$\boldsymbol{L}_0^{(1)} = \frac{\partial^2 \mathscr{F}}{\partial \mathscr{U}_1^2}(0, c_0) = \mathrm{diag}\left[0, 0, \frac{k}{\rho + \rho'}, \frac{k}{\rho + \rho'}\right],$$

$$\boldsymbol{L}_0^{(n)} = \frac{\partial^2 \mathscr{F}}{\partial \mathscr{U}_n^2}(0, c_o) = \mathrm{diag}\left[-\beta_n, -\beta_n, \frac{nk}{\rho + \rho'}, \frac{nk}{\rho + \rho'}\right] \quad n = 2, \ldots, N\,.$$

Clearly, $\boldsymbol{L}_0$ has two zero eigenvalues. The other $4N-2$ eigenvalues of $\boldsymbol{L}_0$ are positive if $\beta_n < 0$ for $n \geqslant 2$. Recall from equation (2.38) that $\beta_n$ is given by

$$\beta_n = -(\rho - \rho')g + \left(\frac{\rho\rho'}{\rho + \rho'}\frac{u^2}{k} - n\sigma\right) nk^2$$

but at the KH instability point,

$$(\rho - \rho')g = \tau\sigma k^2 \quad \text{and} \quad \rho\rho' k u^2/(\rho + \rho') = (\tau + 1)\sigma k^2\,.$$

Therefore

$$-\beta_n = (n-1)(n-\tau)\sigma k^2\,.$$

With the restrictions $n \geqslant 2$ and $0 < \tau < 2$ it is clear that $-\beta_n > 0$, verifying that $\boldsymbol{L}_0$ has $4N-2$ positive eigenvalues.

Application of the result in (3.13) requires an expression for the impulse along a solution branch. The impulse in matrix form was given in equation (2.29). Combining

(2.29) with the expression for the vector $\widehat{\boldsymbol{\zeta}}$ given in (2.34) the impulse is

$$I = -(c-c_0)\boldsymbol{R}'^{T}\boldsymbol{J}\boldsymbol{P}\boldsymbol{J}\boldsymbol{R}' - \frac{\rho\rho'}{\rho+\rho'}u\boldsymbol{R}'^{T}\boldsymbol{J}[\boldsymbol{P}^{+}-\boldsymbol{P}^{-}]\boldsymbol{J}\boldsymbol{R}', \tag{3.16}$$

where $\boldsymbol{R}'$ is defined in (2.15) and explicit expressions for the matrices $\boldsymbol{P}^{\pm}$ are given in Appendix A. For $N=3$ the expression in (3.16) can be simplified to

$$I = (\rho+\rho')k(c-c_0)(A_1^2+B_1^2) - 2\frac{\rho\rho'}{\rho+\rho'}uk^2[A_2(A_1^2-B_1^2)+2A_1B_1B_2]+\cdots.$$

Substitute for $A_2$ and $B_2$ using (2.40), let $z=k^2(A_1^2+B_1^2)$ and use the constants $h^0_{cc}$ and $h^0_{zc}$ defined in (2.50) and (2.62), then

$$I = \frac{1}{2k^2}\left[h^0_{cc}(c-c_0)\,z + \tfrac{1}{2}h^0_{zc}z^2+\cdots\right]. \tag{3.17}$$

Differentiating $I$ with respect to $c$: $\mathrm{d}I/\mathrm{d}c = I_c + I_z z_c$, with $z_c$ obtained by differentiating $h(z,c,u,r)=0$: $z_c=-h_c/h_z$, results in the following interesting expression for the SH stability index:

$$\Delta_{SH}(z,c,u,r) = -h_z\frac{\mathrm{d}I}{\mathrm{d}c} = I_z h_c - I_c h_z = \det\begin{vmatrix} h_c & h_z \\ I_c & I_z \end{vmatrix}. \tag{3.18}$$

To summarize, the analysis has shown that, locally, all existing branches of periodic travelling waves are given by the zeros of the scalar function $h(z,c,u,r)$ in (2.49) and the SH stability type for the waves is determined by the sign of the second scalar function $\Delta_{SH}(z,c,u,r)$: $\Delta_{SH}>0$ ($\Delta_{SH}<0$) corresponds to stability (respectively instability).

### 3.3. *SH instability when $r \neq r_o$*

When $r \neq r_0$ the reduced function $h(z,c,u,r)$ simplifies to

$$h(z,c,u,r) = \tfrac{1}{2}h^0_{cc}(c-c_o)^2 + h^0_z z + h^0_u(u-u_0)+\cdots,$$

where expressions for $h^0_{cc}$, $h^0_z$ and $h^0_u$ are given in (2.50)–(2.52). In this case the impulse simplifies to

$$I = \frac{1}{2k^2}h^0_{cc}(c-c_0)z+\cdots$$

(the higher-order terms in $I$ may be retained but will not change the local bifurcation results qualitatively). The SH stability index in (3.18) becomes

$$\Delta_{SH} = I_z h_c - I_c h_z = \frac{1}{2k^2}h^0_{cc}\left[h^0_{cc}(c-c_0)^2 - h^0_z z\right]+\cdots. \tag{3.19}$$

When $r \neq r_0$ then $\mathrm{sign}(h^0_z) = \mathrm{sign}(r-r_0)$ and $\mathrm{sign}(h^0_{cc}) = +1$ always, therefore $\Delta_{SH}$ is positive definite when $r<r_0$, but when $r>r_0$ the index $\Delta_{SH}$ is positive only if

$$z < \frac{h^0_{cc}}{h^0_z}(c-c_0)^2. \tag{3.20}$$

Application of the above result to figure 5 verifies that the branches for $r<r_0$ are SH stable whereas the globally connected branches occurring when $r>r_0$ and $u<u_0$ become SH unstable at finite amplitude as shown in figure 5.

Since changes of SH stability occur when $\mathrm{d}I/\mathrm{d}c$ changes sign there is some advantage in plotting the bifurcation diagrams in $(I,c)$- or $(H,c)$-space. When $r \neq r_o$ the

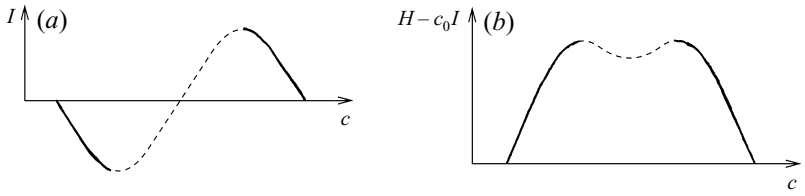


FIGURE 14. Energy and impulse invariants versus wave speed along the branch of TWs in figure 5 when $r > r_0$ and $u < u_0$ with (*a*) impulse and (*b*) shifted energy: $H - c_0 I$.

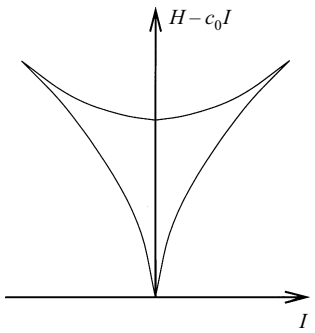


FIGURE 15. Image of $(H(c) - c_o I(c), I(c))$ along the branch of TWs in figure 5 in energy–impulse space.

impulse simplifies to $I = (1/k)(\rho + \rho')(c - c_0)z + \cdots$. With $u$ fixed, $z$ can be considered as a function of $c$ by inverting $h = 0$, resulting in

$$I = \frac{\rho + \rho'}{k h_z^0}(c - c_0)\left(-h_u^0(u - u_0) - \tfrac{1}{2}h_{cc}^0(c - c_0)^2\right) + \cdots . \tag{3.21}$$

The impulse is plotted as a function of $c$ in figure 14(*a*). The unstable branches in figure 5 are clearly associated with a positive slope of $\mathrm{d}I/\mathrm{d}c$ (since in this case $h_z^0 > 0$). Note that the TWs when $c < c_0$ ($c > c_0$) are negative (respectively positive) impulse waves.

The leading-order expression for the total disturbance energy along a branch of TWs is

$$H = c_0 I + \frac{1}{2k^2}[k(\rho + \rho')(c - c_0)^2 - h_u^0(u - u_0)]z - \frac{1}{4k^2}h_z^0 z^2 + \cdots .$$

Again, considering $u$ fixed and inverting $h = 0$, to obtain $z$ as a function of $c$, $H$ can be considered as a function of $c$:

$$H = c_0 I + \frac{1}{4h_z^o k^2}\left[(h_u^0)^2(u - u_0)^2 - 2h_u^0 k(\rho + \rho')(u - u_0)(c - c_0)^2 - 3k^2(\rho + \rho')^2(c - c_0)^4\right] + \cdots$$

with $I$ given in (3.21). The shifted energy, $H - c_0 I$, is plotted in figure 14(*b*) as a function of $c$ along the global branch in figure 5. The two changes of stability along the branch occur when $\mathrm{d}H/\mathrm{d}c = 0$.

The pictures in figures 14(*a*) and 14(*b*) can be combined into a single figure in energy-impulse space. The two functions $H(c) - c_0 I(c)$ and $I(c)$ parameterize a curve in $(H, I)$ space which turns out to be a cut through the swallowtail singularity as shown in figure 15. The interesting feature of figure 15 is that the changes of SH stability

for the TWs arise as cusp singularities in energy–impulse space! It is interesting to compare figure 15 with figure 6 which was obtained using Drazin's modulation equation. Note also that the swallowtail singularity in figure 15 is precisely what occurs in a normalized Hamiltonian system in the neighbourhood of a collision of purely imaginary eigenvalues when plotted in energy–momentum space (see van der Meer 1985, p. 79).

The change of SH stability along a branch is the dominant qualitative feature in figure 5 when $r > r_0$ and $u < u_0$. The SH unstable branch occurs for all density ratios satisfying $r > r_0$ and in an open neighbourhood of the KH neutral curve and it occurs at low amplitude, with the amplitude scaling like $(u_0-u)^{1/2}$ as $u \to u_0$. Therefore, since SH instability has been shown to lead to wave breaking in the classic water-wave problem, and KH roll-up is form of wave breaking, it is natural to propose SH instability as a new mechanism for the formation of KH billows, in the region of parameter space just before ($u < u_0$) the KH threshold.

### 3.4. *SH instability when* $r \approx r_0$

When $r \approx r_0$ it was shown in §2.5 that higher-order terms need to be retained in $h$; we found that

$$h = \tfrac{1}{2}h^0_{cc}(c-c_0)^2 + h^0_{cz}(c-c_0)z + \tfrac{1}{2}h^0_{zz}z^2 + h^0_{rz}(r-r_0)z + h^0_u(u-u_0) + \cdots$$

(with the coefficients defined in expressions (2.61)–(2.63)) from which it follows that

$$\begin{aligned} h_c &= h^0_{cc}(c-c_0) + h^0_{cz}z + \cdots, \\ h_z &= h^0_{cz}(c-c_0) + h^0_{zz}z + h^0_{rz}(r-r_0) + \cdots . \end{aligned}$$

Dropping the $\frac{1}{2}k^{-2}$ factor in the expression (3.17) for the impulse (which does not affect the sign of $\Delta_{SH}$) it follows that

$$\begin{aligned} I_c &= h^0_{cc}z + \cdots, \\ I_z &= h^0_{cc}(c-c_0) + h^0_{cz}z + \cdots . \end{aligned}$$

Note that $I_z = h_c$ to the order shown. The expression (3.18) for the SH stability index is therefore

$$\Delta_{SH} = \left[h^0_{cc}(c-c_0) + h^0_{cz}z\right]^2 - h^0_{cc}z\left[h^0_{cz}(c-c_0) + h^0_{zz}z + h^0_{rz}(r-r_0)\right].$$

Introduce the scaling that was used in §2.5: $\tilde{z} = z\left(\frac{1}{2}|h^0_{zz}|\right)^{1/2}$, $\tilde{c}-\tilde{c}_0 = (c-c_0)\left(\frac{1}{2}|h^o_{cc}|\right)^{1/2}$ and $(\tilde{r}-\tilde{r}_0)(2|h^0_{zz}|)^{1/2} = h^0_{rz}(r-r_0)$. Then using $m$ as defined in (2.66) $\Delta_{SH}$ is transformed to

$$\Delta_{SH} = 2h^0_{cc}\left[(\tilde{c}-\tilde{c}_0)^2 + m\tilde{z}(\tilde{c}-\tilde{c}_0) + (m^2-\epsilon)\tilde{z}^2 - (\tilde{r}-\tilde{r}_0)\tilde{z}\right],$$

with $\epsilon = \pm 1$ as defined in equation (2.64). For simplicity the tildes are dropped in the further discussion of the above expression. Noting also that the factor $2h^0_{cc}$ does not affect the sign of $\Delta_{SH}$, the SH stability index for TWs near the point $(u_0, r_0)$ simplifies to

$$\Delta_{SH} = (c-c_0)^2 + m(c-c_0)z + (m^2-\epsilon)z^2 - (r-r_0)z\,. \tag{3.22}$$

A solution $(z,c)$ of $h(z,c,u,r) = 0$ is SH stable if $\Delta_{SH}(z,c,u,r) > 0$ and SH unstable if $\Delta_{SH}(z,c) < 0$. Setting $\Delta_{SH} = 0$ results in a curve in the $(|\boldsymbol{x}|,c)$-plane separating regions of stable and unstable type. Changes of stability along a branch will occur at points that satisfy $h = 0$ and $\Delta_{SH} = 0$ simultaneously.

Some general observations about $\Delta_{SH}$ can be made. Recast equation (3.22) as

$$\Delta_{SH} = \left[(c - c_0) + \tfrac{1}{2}mz\right]^2 + (\tfrac{3}{4}m^2 - \epsilon)z^2 - (r - r_0)z\,. \tag{3.23}$$

In §2.5 it was shown that $m^2 > 1$ for all $\tau \in (0, 2)$ (see definition for $m$ in (2.66)). In fact it is easy to show that $m^2 > 4/3$ for all $\tau \in (0, 2)$ (for example $m^2 \approx 2.21$ when $\tau = 1$). Therefore, $\frac{3}{4}m^2 - \epsilon > 0$ and it follows from (3.23) that $\Delta_{SH}$ is positive definite if $r < r_0$; that is, all TWs are SH stable when $r < r_0$.

A second observation is that $\Delta_{SH} = 0$ forms a closed compact curve in the $(|x|, c)$-plane that always intersects the point $(0, c_0)$. This is seen by noting that $(\frac{3}{4}m^2 - \epsilon) > 0$ and recasting (3.23) as

$$\Delta_{SH} = \left[(c - c_0) + \tfrac{1}{2}mz\right]^2 + (\tfrac{3}{4}m^2 - \epsilon)\left(z - \frac{1}{2}\frac{(r - r_0)}{(\frac{3}{4}m^2 - \epsilon)}\right)^2 - \frac{1}{4}\frac{(r - r_0)^2}{(\frac{3}{4}m^2 - \epsilon)}\,.$$

Note also that $\Delta_{SH}$ is negative in the region interior to the curve $\Delta_{SH} = 0$ and furthermore, when $r > r_0$, the region enclosed by the curve grows with increasing $r - r_0$. Therefore any solution of $h = 0$ passing through the interior (exterior) of the curve $\Delta_{SH} = 0$ is of unstable (respectively stable) type.

The solution sets of $h = 0$ depend on whether $\epsilon = \pm 1$ and furthermore depend on the region in the $(u, r)$-plane (figures 8 and 10). In figures 9 and 11 the branches of TWs with $\Delta_{SH} < 0$ ($\Delta_{SH} > 0$) are SH unstable (SH stable) and are marked with dashed lines (respectively solid lines).

When $r \leqslant r_0$ the curve $\Delta_{SH} = 0$ is simply the point $(0, c_0)$, since, from (3.23), $\Delta_{SH} = 0$ implies $(r - r_0)z \geqslant 0$, so the only solution when $r < r_0$ is $z = 0$. However, for $r > r_0$, the curve $\Delta_{SH} = 0$ grows as $r$ is increased. A critical value of $r$ (say $\hat{r}$) is reached with

$$r_0 < \hat{r} < r_0 + [-(m^2 - 1)(u - u_0)]^{1/2}$$

when the region $\Delta_{SH} < 0$ first intersects a branch of solutions. This curve is marked as $\mathscr{S}_1$ in figures 8 and 10. For $r > \hat{r}$ and $u < u_0$ some solutions of $h = 0$ pass through the interior of $\Delta_{SH} = 0$ resulting in SH unstable TWs. Note that the detached branches in figures 9 and 11 are SH stable and furthermore the globally connected branches for $r \gg r_0$ have stability assignments in agreement with figure 5. The detached branches of TWs that persist into component (5) of figure 8 or 10 (component (5) corresponds to $u > u_0$ where the equilibrium state is KH unstable) are SH stable.

### 3.5. *Intersection of branches of positive- and negative-energy TWs*

In crossing from region (2) to (3) in figure 8 and from region (3) to (4) in figure 10 a bifurcation point occurs. There is an exact intersection of two branches of TWs. The exact intersection of the two branches exists along a line in $(u, r)$-space: by perturbing the density ratio the branches break apart as shown in the bifurcation diagrams for regions (2) and (3) in figure 9 and regions (3) and (4) in figure 11. However the changes of stability are interesting along this line in parameter space and furthermore the SH stability index $\Delta_{SH}$ reduces to a particularly simple and illuminating form.

For the transversal intersection of branches to occur at some point $P$ in the $(c, |\boldsymbol{x}|)$-plane, it is necessary that the reduced function $h(z, c, u, r)$ given below equation (2.68) satisfies $h = h_z = h_c = 0$ at $P$. The equations $h_z = h_c = 0$ are easily solved as

$$c - c_0 = -\frac{m}{m^2 - \epsilon}(r - r_0) \quad \text{and} \quad z = \frac{1}{m^2 - \epsilon}(r - r_0)$$

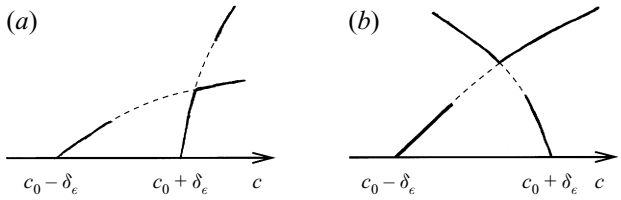


FIGURE 16. Intersection of TW branches along the curve $\mathscr{B}_1$ in figures 8 and 10 with (*a*) $\epsilon = +1$ and (*b*) $\epsilon = -1$. SH stable (unstable) branches are indicated by solid (dashed) lines.

under the circumstances, and with the additional necessary conditions for the appropriate region of parameter space,

$$r > r_0\,, \quad u - u_0 < 0\,, \quad h = 0 \text{ reduces to } \quad (r - r_0)^2 + (m^2 - \epsilon)(u - u_0) = 0\,. \tag{3.24}$$

The condition (3.24) is the curve $\mathscr{B}_1$ in figures 8 and 10 and it represents the curve in parameter space for which transversal intersection of the branches in $(c, |\boldsymbol{x}|)$-space can occur. For parameter values satisfying this, $h = 0$ now reduces to

$$h = (c - c_0 + mz)^2 - (m^2 - \epsilon)\left(z - \frac{(r - r_0)}{m^2 - \epsilon}\right)^2 = 0$$

which describes the branches in the $(c, |\boldsymbol{x}|)$-plane, and is solved as

$$c - c_0 = \mp\delta_\epsilon + [-m \pm (m^2 - \epsilon)^{1/2}]z \quad \text{where} \quad \delta_\epsilon \stackrel{\text{def}}{=} \frac{r - r_0}{(m^2 - \epsilon)^{1/2}}\,. \tag{3.25}$$

The two curves in (3.25) form two intersecting parabolas in the $(c, |\boldsymbol{x}|)$-plane as shown in figure 16(*a*) (for $\epsilon = +1$) and figure 16(*b*) (for $\epsilon = -1$). The stability results along the branches are obtained by substituting (3.25) into the SH stability index; we find

$$\Delta_{SH}^{\pm} = (m^2 - \epsilon)^{1/2}\left(z - \frac{r - r_0}{m^2 - \epsilon}\right)\left((2(m^2 - \epsilon)^{1/2} \mp m)z - \delta_\epsilon\right)\,. \tag{3.26}$$

The function $\Delta_{SH}^{\pm}$ changes sign twice along each branch and when $\Delta_{SH}^{\pm}$ is positive it indicates that the TW is SH stable. The bifurcation points $z = (r - r_0)/(m^2 - \epsilon)$ correspond to a change in SH stability type. In addition there is a change in SH stability at

$$z_\pm = \frac{\delta_\epsilon}{(2(m^2 - \epsilon)^{1/2} \mp m)},$$

where the upper sign corresponds to the left branch and the lower corresponds the right-hand branch. Note that the bifurcation points $z_\pm$ depend linearly on $|r - r_o|$ and arise out of the singularity $r = r_o$. Using the fact that $m^2 > 4/3$ and $m < -1$ the stability assignments are as shown in figure 16.

The bifurcation point occurs in parameter space when the identity (3.24) is met exactly. The expression in (3.24) is in scaled coordinates but is essentially a relation between $r$ (the density ratio) and $u$ (the relative velocity) that depends on $\tau$. It is a parabola in the $(u, r)$-plane as shown in figures 8 and 10 (the $\mathscr{B}_1$ curve). Therefore, there exists a physically realizable value of the fluid density ratio, for each given value of $u \approx u_0$ but $u < u_0$, at which the two bifurcating branches of periodic TWs intersect transversely, with SH stability properties qualitatively similar to those shown in figure 16.

## 4. Interaction between the BF instability and KH instability

The BF instability corresponds to the loss of stability of a Stokes' TW to sideband perturbations (cf. Benjamin & Feir 1967). The critical feature of this instability is that the class of perturbations has a wavelength which is different from that of the basic TW. A rigorous proof of the BF instability for the Stokes' TW, when the fluid depth is sufficiently large, has been given by Bridges & Mielke (1995). For interfacial waves, without a basic velocity difference, a comprehensive analytical treatment of the BF instability is given in Grimshaw & Pullin (1985), with numerical results for large amplitude in Pullin & Grimshaw (1985). Numerical results on BF instability of interfacial gravity waves with a velocity difference are given in Yuen (1985). In this section we consider, formally, the BF instability for bifurcating TWs near a KH unstable equilibrium, with particular interest in the case where the branches of TWs are globally connected and have both SH and BF instabilities at low amplitude.

### 4.1. *BF unstable TWs near the KH unstable equilibrium*

There are a variety of approaches to the analysis of the BF instability (Benjamin & Feir's Fourier theory, nonlinear Schrödinger equation model, Whitham modulation theory, Zakharov equation, etc.). Here we will apply the Whitham–Lighthill instability criterion, based on the Whitham modulation theory, since this analysis fits in well with the Hamiltonian formulation of the KH problem.

The Whitham–Lighthill instability criterion is stated as follows (cf. Whitham (1974)). Let $\mathscr{A}(\omega,k)$ and $\mathscr{B}(\omega,k)$ be the action and action flux respectively evaluated at a TW. Then the particular TW is BF unstable if

$$\Delta_{BF} \stackrel{\text{def}}{=} \det \begin{vmatrix} \mathscr{A}_\omega & \mathscr{A}_k \\ \mathscr{B}_\omega & \mathscr{B}_k \end{vmatrix} > 0 . \tag{4.1}$$

That $\Delta_{BF} > 0$ implies BF instability of the TW is formally established using the Whitham modulation theory (cf. Whitham 1974, Chap. 14).

To apply the criterion (4.1), a definition for $\mathscr{A}(\omega,k)$ and $\mathscr{B}(\omega,k)$ is needed in the context of the Hamiltonian structure of the KH problem. First suppose that $\eta(x,t)$ and $\zeta(x,t)$ are evaluated on a periodic TW, in particular are functions of $\theta = kx-\omega t$. The action for the KH problem was defined in I, §4.4. Averaging the action with respect to $\theta$ and introducing a minus sign (since $\theta_t = -\omega$), we have

$$\mathscr{A}(\omega,k) = -\frac{1}{\pi}\int_0^{2\pi} \zeta\eta_\theta \,\mathrm{d}\theta . \tag{4.2}$$

Treating the least-action functional $\int_{t_1}^{t_2}(H-A)\mathrm{d}t$ (cf. I, §4.4) as a Lagrangian, the action flux is obtained from $\mathscr{B}(\omega,k) = \overline{L}_k = \overline{H}_k$ where $\overline{H}$ is the total energy averaged with respect to $\theta$. From the definitions of $K$ and $V$ in equations (2.2) and (2.3) we have

$$\begin{aligned}\overline{H}(\omega,k) = \frac{1}{\pi}\int_0^{2\pi} &\left[\int_{-\infty}^{\eta} \tfrac{1}{2}\rho(k^2\phi_\theta^2+\phi_y^2)\,\mathrm{d}y + \int_{\eta}^{\infty} \tfrac{1}{2}\rho'(k^2\phi_\theta'^2+\phi_y'^2)\,\mathrm{d}y\right]\mathrm{d}\theta \\ &+\frac{1}{\pi}\int_0^{2\pi} k(-\rho U\Phi+\rho' U'\Phi')\eta_\theta\,\mathrm{d}\theta \\ &+\frac{1}{\pi}\int_0^{2\pi} \left[\tfrac{1}{2}(\rho-\rho')g\eta^2+\sigma((1+k^2\eta_\theta^2)^{1/2}-1)\right]\mathrm{d}\theta\end{aligned}$$

and therefore

$$\mathscr{B}(\omega,k)=\frac{1}{\pi}\int_0^{2\pi}\left[\rho k\int_{-\infty}^{\eta}\phi_\theta^2\,\mathrm{d}y+\rho' k\int_{\eta}^{\infty}\phi_\theta'^2\,\mathrm{d}y\right]\mathrm{d}\theta$$
$$+\frac{1}{\pi}\int_0^{2\pi}\left[(-\rho U\Phi+\rho' U'\Phi')\eta_\theta+\frac{\sigma k\eta_\theta^2}{(1+k^2\eta_\theta^2)^{1/2}}\right]\mathrm{d}\theta\,. \tag{4.3}$$

It is now straightforward to substitute the Fourier expansions into $\mathscr{A}(\omega,k)$ and $\mathscr{B}(\omega,k)$. After some algebra we obtain

$$\left.\begin{aligned}\mathscr{A}(\omega,k)&=-\tfrac{1}{4}D_\omega(\omega,k)(A_1^2+B_1^2)+\cdots,\\ \mathscr{B}(\omega,k)&=-\tfrac{1}{4}D_k(\omega,k)(A_1^2+B_1^2)+\cdots,\end{aligned}\right\} \tag{4.4}$$

where

$$D(\omega,k)=\frac{\rho}{k}(\omega-kU)^2+\frac{\rho'}{k}(\omega-kU')^2-(\rho-\rho')g-\sigma k^2 \tag{4.5}$$

and the nonlinear dispersion relation is

$$D(\omega,k)+k^2v_1(A_1^2+B_1^2)+\cdots=0\,. \tag{4.6}$$

The dispersion relation $D(\omega,k)$ in (4.5) is exactly the expression in the equation below (2.49) but with $c$ replaced by $\omega/k$ and (4.6) is precisely (2.49) with $D$ now treated as a function of $\omega$ and $k$.

In the remainder of this subsection, the BF instabilities of the bifurcating TWs near the KH instability are considered when $r>r_0$ and $k\approx k_0$ where $k_0$ is the minimum point on the KH neutral curve (cf. $\tau=1$ on figure 2),

$$k_0=\left(\frac{(\rho-\rho')g}{\sigma}\right)^{1/2}\quad\text{and}\quad\omega_0=c_0k_0,$$

with $c_0$ as defined in (1.15). In the neighbourhood of $(\omega_0,k_0,u_0)$ the dispersion relation takes the form

$$D(\omega,k)=D_u^0(u-u_0)+\tfrac{1}{2}D_{\omega\omega}^0(\omega-\omega_0)^2+D_{\omega k}^0(\omega-\omega_0)(k-k_0)+\tfrac{1}{2}D_{kk}^0(k-k_0)^2+\cdots \tag{4.7}$$

with

$$D_u^0=\frac{2\rho\rho' k_0u_0}{\rho+\rho'}>0\,,\quad D_{\omega\omega}^0=2\frac{\rho+\rho'}{k_0}>0$$

$$D_{\omega k}^0=-2\frac{\omega_0}{k_0^2}(\rho+\rho')<0\quad\text{and}\quad D_{kk}^0=\frac{2(\rho+\rho')\omega_0^2}{k_0^3}-2\sigma\,.$$

Note in particular that

$$\vartheta^2\overset{\text{def}}{=}-\begin{vmatrix}D_{\omega\omega}^0 & D_{\omega k}^0\\ D_{k\omega}^0 & D_{kk}^0\end{vmatrix}=\frac{4\sigma}{k_0}(\rho+\rho')>0\,. \tag{4.8}$$

We are now in a position to evaluate $\Delta_{BF}$ in (4.1). Dividing $\mathscr{A}$ and $\mathscr{B}$ by $-\frac{1}{4}$ (which does not affect the sign of $\Delta_{BF}$), we find

$$\Delta_{BF}=\frac{z}{k_o^4v_1}\left\{v_1z\begin{vmatrix}D_{\omega\omega} & D_{\omega k}\\ D_{k\omega} & D_{kk}\end{vmatrix}+\begin{vmatrix}D_{\omega\omega} & D_{\omega k} & D_\omega\\ D_{k\omega} & D_{kk} & D_k\\ D_\omega & D_k & 0\end{vmatrix}\right\}+\cdots$$

where $\mathrm{sign}(v_1) = \mathrm{sign}(r - r_o)$ and $z = k_o^2(A_1^2 + B_1^2)$. Since

$$\begin{vmatrix} D_{\omega\omega} & D_{\omega k} & D_\omega \\ D_{k\omega} & D_{kk} & D_k \\ D_\omega & D_k & 0 \end{vmatrix} = D_\omega^3 \frac{\mathrm{d}c_g}{\mathrm{d}k}$$
$$= \vartheta^2[D^0_{\omega\omega}(\omega-\omega_0)^2 + 2D^0_{\omega k}(\omega-\omega_0)(k-k_0) + D^0_{kk}(k-k_0)^2] + \cdots,$$

where $c_g$ is the group velocity, the BF-stability index can be written in the form

$$\Delta_{BF} = \frac{z\vartheta^2}{k_0^4 v_1}(-v_1 z + D^0_{\omega\omega}(\omega-\omega_0)^2 + 2D^0_{\omega k}(\omega-\omega_0)(k-k_0) + D^0_{kk}(k-k_0)^2) + \cdots. \tag{4.9}$$

This index is now applied to the branch of TWs in figure 5 when $r > r_0$ and $u < u_0$ in order to verify the results in figure 4. First, since $v_1 > 0$ for $r > r_0$, as $z \to 0$

$$\mathrm{sign}(\Delta_{BF}) = \mathrm{sign}[D^0_{\omega\omega}(\omega-\omega_0)^2 + 2D^0_{\omega k}(\omega-\omega_0)(k-k_0) + D^0_{kk}(k-k_0)^2]$$
$$= \mathrm{sign}[D^0_u(u_0-u)] > 0$$

for $(|\omega_0-\omega|, |k-k_0|, |u-u_0|)$ sufficiently small. Therefore, it follows that $\Delta_{BF} > 0$ for $z$ sufficiently small when $u < u_0$, verifying that the branches of TWs are BF unstable at low amplitude. However there exists a critical value of the amplitude at which $\Delta_{BF} = 0$ and this amplitude is lower than (or possibly equal to) the amplitude at which SH instability occurs, verifying the stability assignments in figure 4.

As $k \to k_0$ the change of BF instability coalesces with the change of SH instability and furthermore as $u \to u_0$ these two instabilities coalesce with the KH instability.

Along the branch of TWs in figure 4 there is a region of 'stability'. The word stability is in quotes because the wave is BF and SH stable but could be unstable to finite-wavelength disturbances. For example, it is now well known that when the BF instability stabilizes a band of unstable wavenumbers may persist but no longer limits on zero wavenumber (cf. the shift of the band of unstable wavenumbers along the $p$-axis in figures 2($c$) and 2($d$) of McLean 1982).

There is an additional interesting feature that appears in figure 4 which seems to be a general property of wave instabilities. First note that $\mathscr{A}_\omega = 0$ at a change of SH instability where $\mathscr{A}_\omega$ is the partial derivative of $\mathscr{A}$ with respect to $\omega$ with the wavenumber fixed. This can be argued from a number of viewpoints: for example, $H_c = 0$ is equivalent to $H_\omega = 0$ when $k$ is fixed, and from the least-action principle it follows that $H_\omega = 0$ implies $\mathscr{A}_\omega = 0$. Since $\mathscr{A}_k = \mathscr{B}_\omega$ in (4.1) it follows that, generically (assuming $\mathscr{A}_k \neq 0$), at a change of SH stability

$$\Delta_{BF} = -\mathscr{A}_k^2 < 0.$$

Therefore, if along a branch of TWs there is a BF instability at a particular amplitude (implying $\Delta_{BF} > 0$), and at another amplitude there is a change in SH instability (implying $\Delta_{BF} < 0$), then by the intermediate-value theorem there is a point in between at which $\Delta_{BF} = 0$. This property is clearly evoked in figure 4 and also occurs in the classic water-wave problem in deep water, where at low amplitude the Stokes' TW is BF unstable and at large amplitude there is an SH instability.

### 4.2. *Weissman's theory and space–time modulation equations*

The interaction between the BF instability and the SH instability along a branch of TWs near the KH instability can also be obtained from Weissman's space-time modulation equation. Weissman (1979), using a multiple-scale perturbation analysis, showed that the relevant model partial differential equation near the KH instability,

in the neighbourhood of the minimum point of the KH neutral curve, takes the form

$$\frac{\partial^2 A}{\partial T^2} = \vartheta^2 \frac{\partial^2 A}{\partial X^2} - \alpha A + a|A|^2 A, \tag{4.10}$$

where $X$ and $T$ are slow space and time scales, $\mathrm{sign}(\alpha) = \mathrm{sign}(u_0 - u)$ and $\mathrm{sign}(a) = \mathrm{sign}(r - r_o)$. The positive real parameter $\vartheta^2$ is as defined in equation (4.8) (although Weissman 1979, equation (2.21b) normalizes it by dividing by $D^0_{\omega\omega}{}^2$). When $\vartheta = 0$ equation (4.9) reduces to Drazin's time-modulation equation (2.55). Weissman considers many solutions of (4.10) including numerical solutions but surprisingly does not consider the BF or sideband instability. Here we show that equation (4.10) contains the critical picture, figure 4, and includes both the SH instability and BF instability of branches of TWs.

The basic TW solution of (4.10) is

$$A(X,T) = A_0 \mathrm{e}^{\mathrm{i}(kX+\omega T)} \quad \text{with} \quad \omega^2 - \vartheta^2 k^2 + a|A_0|^2 = \alpha\,. \tag{4.11}$$

For purposes of the present subsection, we take $a > 0$ and $\alpha > 0$. To analyse the linear stability of the basic state (4.11), let

$$A(X,T) = (A_0 + B(X,T))\mathrm{e}^{\mathrm{i}(kX+\omega T)}\,;$$

then $B(X,T)$ satisfies

$$B_{TT} + 2\mathrm{i}\omega B_T - \vartheta^2 B_{XX} - 2\mathrm{i}\vartheta^2 k B_X = a(|A_0|^2 B + A_0^2 \overline{B})\,.$$

With $B(X,T) = B_1 \mathrm{e}^{\mathrm{i}(pX+\Omega T)} + B_2 \mathrm{e}^{-\mathrm{i}(pX+\overline{\Omega} T)}$, where $p \in \mathbb{R}$ is the sideband exponent and $\Omega \in \mathbb{C}$ is the stability exponent, we find the following characteristic equation for $\Omega$:

$$\Omega^4 - 2(\vartheta^2 p^2 - a|A_0|^2 + 2\omega^2)\Omega^2 + 8\vartheta^2 \omega k p \Omega + \vartheta^2 p^2 [\vartheta^2 p^2 - 2a|A_0|^2 - 4\vartheta^2 k^2] = 0\,. \tag{4.12}$$

The SH instability is recovered by taking $p = 0$, reducing (4.12) to

$$\Omega^4 - 2(2\omega^2 - a|A_0|^2)\Omega^2 = 0\,,$$

recovering equation (2.58) (with $\lambda = \mathrm{i}\Omega$). The branch of TWs in (4.11) is therefore SH unstable when $a|A_0|^2 > 2\omega^2$.

For the sideband instability, suppose $p \ll 1$ and let

$$\Omega = p\Omega_1 + O(p^2)\,. \tag{4.13}$$

Then, substituting (4.13) into (4.12) results in

$$(a|A_0|^2 - 2\omega^2)\Omega_1^2 + 4\vartheta^2 k\omega\, \Omega_1 - \vartheta^2(a|A_0|^2 + 2\vartheta^2 k^2) = 0\,. \tag{4.14}$$

The basic wave (4.11) is BF unstable when the discriminant of (4.14) is negative or

$$a\vartheta^2|A_0|^2 \left[-a|A_0|^2 + 2(\omega^2 - \vartheta^2 k^2)\right] > 0\,,$$

recovering the result in (4.9), with appropriate change in notation.

For $a \approx 0$ ($r \approx r_0$), the modulation equation (4.10) is no longer valid. The appropriate model equation in that case is not known and would likely be very complicated. On the other hand the geometric criterion (4.1) extends in a straightforward manner to the case when $r \approx r_0$.

## 5. Concluding remarks

The canonical Hamiltonian structure of the KH problem has been used as an organizing centre for an analysis of nonlinear periodic TWs near the KH instability threshold. Several new and surprising results on the bifurcation of TWs as well as the SH and BF instability of TWs were found.

The SH instability of TWs near the KH threshold was treated in some completeness. An extension of Saffman's theory for the SH instability was introduced, leading to a precise relation between the slope in an impulse–wave-speed diagram and SH unstable eigenvalues. For $r > r_0$ the SH instability is pervasive in the neighbourhood of the KH threshold, and it probably persists at larger amplitude for $u \ll u_0$. For $r \approx r_0$ a complicated structure of bifurcation points, isolated branches and interesting SH stability changes was found, which also probably persists at large amplitude for $r \neq r_0$. The analysis has pointed to several open questions about the precise connection between the SH instability and KH billows, as well as the effect of finite depth and three-dimensionality on the SH instability, in general, and for the KH problem, in particular. For example, in finite depth, the mean flow may have an important effect on the SH instability.

Some results on the BF instability were presented for branches of TWs near the KH instability. The most interesting case is when $r > r_0$ and $u < u_0$ and this case was treated in detail. When $r \approx r_0$ there is a rich bifurcation structure as well as interesting changes of SH stability. Therefore it is reasonable to expect that the changes of BF instability near this singularity will also be quite rich. It is not clear that the analysis of BF instability for TWs near the singularity $r = r_0$ will add to the understanding of the nonlinear KH problem but it is certainly of great fundamental interest. A singularity like $r = r_0$ brings down to low amplitude complicated bifurcations and stability changes that normally occur at large amplitude, and can therefore be studied analytically. An analysis of the interaction between the KH instability, SH instability and BF instability for $r \approx r_0$ would require the simultaneous analysis of the three functions $h$, the bifurcation function, $\Delta_{SH}$, the SH stability function, and $\Delta_{BF}$, the BF stability function, all considered as functions of amplitude, wavenumber and frequency, as well as the parameters $u$ and $r$. Addition of three-dimensionality would then add considerable complexity to such a bifurcation and stability analysis.

The authors are grateful to the referees for a careful reading of Parts 1 and 2 and for helpful suggestions.

## Appendix A. Details of the matrices in §2

In the construction of the Hamiltonian structure in §2, using the variational principle of I, §3.1, the operations on the vectors of Fourier coefficients were done using representative matrices. The details of the matrices needed for this construction as well as the construction of the impulse for the superharmonic instability analysis are recorded here.

### A.1. *The matrices* $\boldsymbol{M}^{\pm}$ *and* $\boldsymbol{\Gamma}^{\pm}$

Explicit expressions for the entries in the matrices $\boldsymbol{M}^{\pm}$ and $\boldsymbol{\Gamma}^{\pm}$ are constructed. The $2N \times 2N$ non-symmetric matrices $\boldsymbol{M}^{\pm}$ are a convenient way to represent the finite-dimensional version of the constraint set $\rho\Phi - \rho'\Phi' = \zeta$ (cf. equation (2.10). With the

partitioning

$$\boldsymbol{M}^{\pm} = \begin{bmatrix} \boldsymbol{M}_1^{+} & \boldsymbol{M}_2^{+} \\ \boldsymbol{M}_3^{+} & \boldsymbol{M}_4^{+} \end{bmatrix}$$

the submatrices $\boldsymbol{M}_j^{\pm}$ $j = 1,\ldots,4$ have entries

$$\begin{aligned}
\boldsymbol{M}^{\pm}_{1\,m,n} &= \frac{2}{\ell}\int_0^{\ell} \mathrm{e}^{\pm nk\eta(x)} \cos mkx \cos nkx \,\mathrm{d}x, \\
\boldsymbol{M}^{\pm}_{2\,m,n} &= \frac{2}{\ell}\int_0^{\ell} \mathrm{e}^{\pm nk\eta(x)} \cos mkx \sin nkx \,\mathrm{d}x, \\
\boldsymbol{M}^{\pm}_{3\,m,n} &= \frac{2}{\ell}\int_0^{\ell} \mathrm{e}^{\pm nk\eta(x)} \sin mkx \cos nkx \,\mathrm{d}x \\
\boldsymbol{M}^{\pm}_{4\,m,n} &= \frac{2}{\ell}\int_0^{\ell} \mathrm{e}^{\pm nk\eta(x)} \sin mkx \sin nkx \,\mathrm{d}x .
\end{aligned}$$

These integrals are evaluated using the following observation. Let

$$\Upsilon_n^{\pm} = \frac{2}{\ell}\int_0^{\ell} \mathrm{e}^{\pm nk\eta(x)} \,\mathrm{d}x$$

with $n$ any positive integer. The wave height $\eta(x)$ is a linear function of its Fourier coefficients and so

$$\frac{\partial \eta}{\partial A_m} = \cos mkx, \qquad \frac{\partial \eta}{\partial B_m} = \sin mkx, \quad m = 1,\ldots,N .$$

Therefore

$$\pm\frac{1}{nk}\frac{\partial \Upsilon_n^{\pm}}{\partial A_m} = \frac{2}{\ell}\int_0^{\ell} \mathrm{e}^{\pm nk\eta(x)} \cos mkx \,\mathrm{d}x, \tag{A 1}$$

$$\pm\frac{1}{nk}\frac{\partial \Upsilon_n^{\pm}}{\partial B_m} = \frac{2}{\ell}\int_0^{\ell} \mathrm{e}^{\pm nk\eta(x)} \sin mkx \,dx . \tag{A 2}$$

The basic observation is that the only integral to be evaluated is $\Upsilon_n^{\pm}$. After integration $\Upsilon_n^{\pm}$ is a polynomial function of the Fourier coefficients $A_j$, $B_j$ $(j = 1,\ldots,N)$, for any finite $N$. The integrals in the matrices $\boldsymbol{M}^{\pm}$ are then obtained by differentiation:

$$\left.\begin{aligned}
\boldsymbol{M}^{\pm}_{1\,m,n} &= \frac{1}{n^2k^2}\frac{\partial^2 \Upsilon_n^{\pm}}{\partial A_m \partial A_n}, & \boldsymbol{M}^{\pm}_{2\,m,n} &= \frac{1}{n^2k^2}\frac{\partial^2 \Upsilon_n^{\pm}}{\partial A_m \partial B_n} \\
\boldsymbol{M}^{\pm}_{3\,m,n} &= \frac{1}{n^2k^2}\frac{\partial^2 \Upsilon_n^{\pm}}{\partial B_m \partial A_n}, & \boldsymbol{M}^{\pm}_{4\,m,n} &= \frac{1}{n^2k^2}\frac{\partial^2 \Upsilon_n^{\pm}}{\partial B_m \partial B_n}
\end{aligned}\right\} \text{ for } m,n = 1,\ldots,N.$$

Letting $N = 3$, and retaining terms to sufficient order to obtain the results in §2 to sixth order, the polynomial $\Upsilon_n^{\pm}$ is

$$\begin{aligned}
\frac{1}{n^2k^2}\Upsilon_n^{\pm} = \frac{2}{n^2k^2} &+ \tfrac{1}{2}(A_1^2 + B_1^2) + \tfrac{1}{2}(A_2^2 + B_2^2) \\
&\pm \tfrac{1}{4}nk[A_2(A_1^2 - B_1^2) + 2A_1B_1B_2] + \tfrac{1}{32}n^2k^2(A_1^2 + B_1^2)^2 \\
&+ \tfrac{1}{8}n^2k^2[A_1^2(A_2^2 + B_2^2 + B_1B_3) + B_1^2(A_2^2 + B_2^2 - A_1A_3)] \\
&\pm \tfrac{1}{48}n^3k^3[A_2(A_1^4 - B_1^4) + 2A_1B_1B_2(A_1^2 + B_1^2)] \\
&+ \tfrac{1}{2}(A_3^2 + B_3^2) + \tfrac{1}{24}n^2k^2(A_1^3A_3 - B_1^3B_3) + \tfrac{1}{1152}n^4k^4(A_1^2 + B_1^2)^3 \\
&\pm \tfrac{1}{2}nk[A_1(A_2A_3 + B_2B_3) + B_1(A_2B_3 - B_2A_3)] + \cdots .
\end{aligned} \tag{A 3}$$

The matrices $\boldsymbol{\Gamma}^{\pm}$, used in the construction of the kinetic energy in §2, can also be characterised in terms of the functions $\Upsilon_n^{\pm}$. The matrices $\boldsymbol{\Gamma}^{\pm}$ are $2N \times 2N$ symmetric matrices that can be partitioned as

$$\boldsymbol{\Gamma}^{\pm} = \begin{bmatrix} \boldsymbol{C}^{\pm} & -\boldsymbol{S}^{\pm} \\ \boldsymbol{S}^{\pm} & \boldsymbol{C}^{\pm} \end{bmatrix},$$

where $\boldsymbol{C}^{\pm}$ are $N \times N$ symmetric matrices and the matrices $\boldsymbol{S}^{\pm}$ are $N \times N$ skew-symmetric matrices. Upon evaluation of the kinetic energy with the finite-dimensional Fourier approximation for each of the velocity components $\phi$ and $\phi'$, it is found that

$$\boldsymbol{C}^{\pm}{}_{m,n} = k\frac{mn}{m+n}\frac{2}{\ell}\int_0^{\ell} \mathrm{e}^{\pm(m+n)k\eta(x)}\cos(m-n)kx\,\mathrm{d}x,$$
$$\boldsymbol{S}^{\pm}{}_{m,n} = k\frac{mn}{m+n}\frac{2}{\ell}\int_0^{\ell} \mathrm{e}^{\pm(m+n)k\eta(x)}\sin(m-n)kx\,\mathrm{d}x.$$

Using (A1) and (A2), the entries of $\boldsymbol{\Gamma}^{\pm}$ can be given in terms of the polynomial $\Upsilon_n^{\pm}$,

$$\boldsymbol{C}^{\pm}{}_{m,n} = \left\{ \begin{array}{ll} \pm\dfrac{mn}{(m+n)^2}\dfrac{\partial \Upsilon^{\pm}_{m+n}}{\partial A_{|m-n|}} & \text{if } m \neq n \\ \frac{1}{2}nk\,\Upsilon^{\pm}_{2n} & \text{if } m = n \end{array} \right\} \quad \text{for } m,n = 1,\ldots,N$$

and

$$\boldsymbol{S}^{\pm}{}_{m,n} = \left\{ \begin{array}{ll} \pm\mathrm{sign}(m-n)\dfrac{mn}{(m+n)^2}\dfrac{\partial \Upsilon^{\pm}_{m+n}}{\partial B_{|m-n|}} & \text{if } m \neq n \\ 0 & \text{if } m = n \end{array} \right\} \quad \text{for } m,n = 1,\ldots,N.$$

The entries of the matrices $\boldsymbol{\Gamma}^{\pm}$ are now easily constructed using $\Upsilon_n^{\pm}$ in (A3).

The inverse of $\boldsymbol{\Gamma}^{\pm}$ is necessary in the reduction of the system of algebraic equations. When $A_j = B_j = 0$ for $j = 1,\ldots,N$ the matrices $\boldsymbol{S}^{\pm}$ are identically zero and the matrices $\boldsymbol{C}^{\pm}$ are diagonal. Therefore, for $A_j$, $B_j$ $j = 1,\ldots,N$, sufficiently small, $\boldsymbol{\Gamma}^{\pm}$ can be considered as a perturbation of a diagonal matrix,

$$\boldsymbol{\Gamma}^{\pm} = \begin{pmatrix} \boldsymbol{C}^{\pm} & -\boldsymbol{S}^{\pm} \\ \boldsymbol{S}^{\pm} & \boldsymbol{C}^{\pm} \end{pmatrix} = \begin{pmatrix} \boldsymbol{C}^{\pm} & 0 \\ 0 & \boldsymbol{C}^{\pm} \end{pmatrix}\left[\begin{pmatrix} \boldsymbol{I} & 0 \\ 0 & \boldsymbol{I} \end{pmatrix} - \begin{pmatrix} 0 & \widehat{\boldsymbol{S}} \\ -\widehat{\boldsymbol{S}} & 0 \end{pmatrix}\right]$$

where $\widehat{\boldsymbol{S}} = \boldsymbol{C}^{\pm -1}\boldsymbol{S}^{\pm}$, and so

$$\boldsymbol{\Gamma}^{\pm -1} = \left[\begin{pmatrix} \boldsymbol{I} & 0 \\ 0 & \boldsymbol{I} \end{pmatrix} + \begin{pmatrix} 0 & \widehat{\boldsymbol{S}} \\ -\widehat{\boldsymbol{S}} & 0 \end{pmatrix} + \begin{pmatrix} 0 & \widehat{\boldsymbol{S}} \\ -\widehat{\boldsymbol{S}} & 0 \end{pmatrix}^2 + \cdots\right]\begin{pmatrix} \boldsymbol{C}^{\pm -1} & 0 \\ 0 & \boldsymbol{C}^{\pm -1} \end{pmatrix}.$$

Retaining terms sufficient for the sixth-order bifurcation equation, the inverse is

$$\boldsymbol{\Gamma}^{\pm -1} = \begin{bmatrix} [\boldsymbol{I} - \widehat{\boldsymbol{S}}^2 + \widehat{\boldsymbol{S}}^4][\boldsymbol{C}^{\pm}]^{-1} & \widehat{\boldsymbol{S}}[\boldsymbol{I} - \widehat{\boldsymbol{S}}^2]\boldsymbol{C}^{\pm -1} \\ -\widehat{\boldsymbol{S}}[\boldsymbol{I} - \widehat{\boldsymbol{S}}^2]\boldsymbol{C}^{\pm -1} & [\boldsymbol{I} - \widehat{\boldsymbol{S}}^2 + \widehat{\boldsymbol{S}}^4]\boldsymbol{C}^{\pm -1} \end{bmatrix}$$

with the explicit entries for $N = 3$ given by

$$[\boldsymbol{I} - \widehat{\boldsymbol{S}}^2 + \widehat{\boldsymbol{S}}^4]\boldsymbol{C}^{\pm -1} = \frac{1}{k}\begin{bmatrix} \hat{\gamma}_{11} & \hat{\gamma}_{12} & \mp kA_2 + k^2(A_1^2 - B_1^2) \\ \hat{\gamma}_{12} & \frac{1}{2}(1 + 4k^2(A_1^2 + B_1^2)) & \mp kA_1 \\ \mp kA_2 + k^2(A_1^2 - B_1^2) & \mp kA_1 & \frac{1}{3} - k^2(A_1^2 + B_1^2) \end{bmatrix},$$

where

$$\hat{\gamma}_{12} = \mp kA_1 \mp \tfrac{9}{8}k^3A_1(A_1^2 + B_1^2) + \tfrac{3}{2}k^2(B_1B_2 + A_1A_2),$$

$$\hat{\gamma}_{11} = 1 + k^2(A_1^2 + B_1^2) + 2k^2(A_2^2 + B_2^2) + \tfrac{1}{4}k^4(A_1^2 + B_1^2)^2 \pm k^3A_2(B_1^2 - A_1^2) \mp 2k^3A_1B_1B_2$$

and

$$\widehat{\boldsymbol{S}}[\boldsymbol{I} - \widehat{\boldsymbol{S}}^2]\boldsymbol{C}^{\pm -1} = \frac{1}{k}\begin{bmatrix} 0 & \theta_{12} & \mp kB_2 + 2k^2A_1B_1 \\ -\theta_{12} & 0 & \mp kB_1 \\ \pm kB_2 - 2k^2A_1B_1 & \pm kB_1 & 0 \end{bmatrix}$$

with

$$\theta_{12} = \mp kB_1 - \tfrac{3}{2}k^2(B_1A_2 - A_1B_2) \mp \tfrac{9}{8}k^3B_1(A_1^2 + B_1^2)\,.$$

### A.2. *The matrices* $\boldsymbol{P}^{\pm}$

The entries in the matrices $\boldsymbol{P}^{\pm}$ that appear in the finite-dimensional expression for the kinetic energy are recorded here. The matrices $\boldsymbol{P}^{\pm}$ are of order $2N$ and symmetric and can be partitioned into

$$\boldsymbol{P}^{\pm} = \begin{bmatrix} \boldsymbol{P}_1^{\pm} & \boldsymbol{P}_2^{\pm} \\ \boldsymbol{P}_3^{\pm} & \boldsymbol{P}_4^{\pm} \end{bmatrix}$$

where $\boldsymbol{P}_1^{\pm}$ and $\boldsymbol{P}_3^{\pm}$ are $N \times N$ symmetric matrices and $\boldsymbol{P}_2^{\pm}$ are $N \times N$ non-symmetric matrices. With $N = 3$ the above matrices take the explicit form

$$\boldsymbol{P}_1^{\pm} = \frac{1}{k}\begin{bmatrix} \boldsymbol{P}_{1\,1,1}^{\pm} & \boldsymbol{P}_{1\,1,2}^{\pm} & 0 \\ \boldsymbol{P}_{1\,1,2}^{\pm} & \frac{1}{2} & 0 \\ 0 & 0 & \frac{1}{3} \end{bmatrix}$$

where

$$\boldsymbol{P}_{1\,1,1}^{\pm} = 1 \pm kA_2 + \tfrac{1}{2}k^2(A_2^2 + B_2^2) + \tfrac{1}{4}k^2(A_1^2 - B_1^2) - \tfrac{1}{2}k^2(A_1A_3 + B_1B_3) \pm \tfrac{1}{2}k^3A_1B_1B_2 \mp \tfrac{3}{4}k^3B_1^2A_2 \pm \tfrac{1}{4}k^3A_2A_1^2 + \tfrac{1}{96}k^4(11B_1^4 + 6A_1^2B_1^2 - 5A_1^4),$$

$$\boldsymbol{P}_{1\,1,2}^{\pm} = \pm kA_3 \pm \tfrac{1}{24}k^3A_1^3 \mp \tfrac{1}{8}k^3A_1B_1^2 + \tfrac{1}{2}k^2A_1A_2 - \tfrac{1}{2}k^2B_1B_2\,.$$

For $\boldsymbol{P}_2^{\pm}$ we find

$$\boldsymbol{P}_2^{\pm} = \frac{1}{k}\begin{bmatrix} \boldsymbol{P}_{2\,1,1}^{\pm} & \boldsymbol{P}_{2\,1,2}^{\pm} & 0 \\ \boldsymbol{P}_{1\,1,2}^{\pm} & 0 & 0 \\ 0 & 0 & 0 \end{bmatrix}$$

where

$$\boldsymbol{P}_{2\,1,1}^{\pm} = \pm kB_2 + \tfrac{1}{2}k^2(B_1A_3 - A_1B_3) + \tfrac{1}{2}k^2A_1B_1, \mp\tfrac{1}{2}k^3(B_2A_1^2 + B_1^2B_2) - \tfrac{1}{6}k^4A_1B_1^3 - -\tfrac{1}{6}k^4A_1^3B_1,$$

$$\boldsymbol{P}_{2\,1,2}^{\pm} = \pm kB_3 + \tfrac{1}{2}k^2(B_1A_2 + A_1B_2) \pm \tfrac{1}{24}k^3(3A_1^2 - B_1^2)A_1\,.$$

For $\boldsymbol{P}_3^{\pm}$ we find

$$\boldsymbol{P}_3^{\pm} = \frac{1}{k}\begin{bmatrix} \boldsymbol{P}_{3\,1,1}^{\pm} & \boldsymbol{P}_{3\,1,2}^{\pm} & 0 \\ \boldsymbol{P}_{3\,1,2}^{\pm} & \frac{1}{2} & 0 \\ 0 & 0 & \frac{1}{3} \end{bmatrix},$$

where

$$\boldsymbol{P}^{\pm}_{3\,1,1} = 1 \mp kA_2 + \tfrac{1}{2}k^2(A_2^2 + B_2^2) - \tfrac{1}{4}k^2(A_1^2 - B_1^2) + \tfrac{1}{2}k^2(A_1A_3 + B_1B_3) \pm \tfrac{1}{2}k^3A_1B_1B_2 \pm \tfrac{1}{12}k^3A_2(9A_1^2 + 3B_1^2) + \tfrac{1}{96}k^4(11A_1^4 + 6A_1^2B_1^2 - 5B_1^4),$$

$$\boldsymbol{P}^{\pm}_{3\,1,2} = \mp kA_3 \pm \tfrac{1}{24}k^3A_1(3B_1^2 - A_1^2) + \tfrac{1}{2}k^2(B_1B_2 - A_1A_2)\,.$$

Note that when $A_j = B_j = 0$ for $j = 1, 2, 3$ the matrix $\boldsymbol{P}^{\pm}$ is a diagonal matrix. Therefore $\boldsymbol{P}^{\pm}$ has a well-defined inverse for $A_1^2 + B_1^2$ sufficiently small.

## Appendix B. Impulse, wave speed and critical point type

In this Appendix the analysis at the end of §3.2 is completed by showing that when the spectrum of $\mathrm{L}(\mathscr{U}, c)$ has the decomposition (3.11) and $\mu_2 \mathrm{d}I/\mathrm{d}c > 0$, where $\mu_2$ is the critical eigenvalue of $\mathrm{L}(\mathscr{U}, c)$ defined in (3.11), (3.12) and Appendix C, the basic TW state is a constrained minimum of the energy and therefore linearly stable. The connection between constrained minima and orbital stability is now well-established in the literature (cf. Benjamin 1972; Oh 1987; Maddocks 1991 and references therein).

Let $\mathscr{U} \in \mathbb{R}^{4N}$ be the vector giving rise to a TW and satisfying

$$\nabla \mathscr{F}(\mathscr{U}, c) = \nabla H(\mathscr{U}) - c\,\nabla I(\mathscr{U}) = 0\,, \tag{B 1}$$

and let

$$\mathrm{L}(\mathscr{U}, c) \stackrel{\mathrm{def}}{=} D^2H(\mathscr{U}) - c\,D^2I(\mathscr{U})\,. \tag{B 2}$$

Suppose the spectrum of $\mathrm{L}(\mathscr{U}, c)$ is decomposed in the form given in equation (3.11) with orthonormalized eigenvectors $\boldsymbol{\xi}_1, \ldots, \boldsymbol{\xi}_{4N}$. The eigenvalue $\mu_1$ is zero with eigenvector $\boldsymbol{\xi}_1$, $\mu_2$ may be positive or negative and $\mu_3, \ldots, \mu_{4N}$ are positive. Under the above conditions on the spectrum of $\mathrm{L}(\mathscr{U}, c)$ we will prove that $\mathscr{U} \in \mathbb{R}^{4N}$ minimizes $H$ on the constraint set $I(\mathscr{U}) = \mathscr{I} \in \mathbb{R}$ when $\mu_2 I_c > 0$. This is proved by showing that the quadratic form $S(\boldsymbol{Y}) = \langle \boldsymbol{Y}, \mathrm{L}(\mathscr{U}, c)\boldsymbol{Y} \rangle$ is strictly positive for all $\boldsymbol{Y}$ such that

$$\langle \boldsymbol{\xi}_1, \boldsymbol{Y} \rangle = 0 \quad \text{and} \quad \langle \nabla I(\mathscr{U}), \boldsymbol{Y} \rangle = 0 \tag{B 3}$$

when

$$\mu_2 \frac{\mathrm{d}I}{\mathrm{d}c} > 0\,.$$

The first condition in (B3) eliminates the zero eigenvalue of $\mathrm{L}(\mathscr{U}, c)$ and the second condition ensures that $\boldsymbol{Y}$ is in the tangent space of the constraint set.

Express the class of admissible variations $\boldsymbol{Y}$ in a spectral expansion

$$\boldsymbol{Y} = \sum_{j=2}^{4N} y_j \boldsymbol{\xi}_j\,. \tag{B 4}$$

Since $\mathrm{L}\boldsymbol{Y} = \sum_{j=2}^{4N} \mu_j y_j \boldsymbol{\xi}_j$ it follows that

$$S(\boldsymbol{Y}) = \mu_2 y_2^2 + \sum_{j=3}^{4N} \mu_j y_j^2\,. \tag{B 5}$$

A critical point $\mathscr{U} \in \mathbb{R}^{4N}$ satisfies $\nabla H(\mathscr{U}) - c\nabla I(\mathscr{U}) = 0$, therefore

$$\frac{\mathrm{d}}{\mathrm{d}c}\{\nabla H(\mathscr{U}) - c\nabla I(\mathscr{U})\} = \mathrm{L}(\mathscr{U}, c)\frac{\mathrm{d}\mathscr{U}}{\mathrm{d}c} - \nabla I(\mathscr{U}) = 0.$$

Since admissible variations $\boldsymbol{Y}$ are required to be orthogonal to $\nabla I(\mathscr{U})$ (cf. equation (B3)),

$$\langle \boldsymbol{Y}, \nabla I(\mathscr{U})\rangle = \langle \boldsymbol{Y}, \mathrm{L}(\mathscr{U}, c)\mathscr{U}_c\rangle = 0. \tag{B 6}$$

Let $\mathscr{U}_c = \sum_{j=2}^{4N} w_j\xi_j$; then $\mathrm{L}(\mathscr{U}, c)\,\mathscr{U}_c = \sum_{j=2}^{4N}\mu_j w_j\boldsymbol{\xi}_j$ and therefore

$$0 = \langle \boldsymbol{Y}, \mathrm{L}(\mathscr{U}, c)\,\mathscr{U}_c\rangle = \sum_{j=2}^{4N}\mu_j y_j w_j$$

or $-\mu_2 y_2 w_2 = \sum_{j=3}^{4N}\mu_j y_j w_j$ resulting in

$$\mu_2 y_2^2 = \frac{\left(\sum\limits_{j=3}^{4N}\mu_j y_j w_j\right)^2}{\mu_2 w_2^2}. \tag{B 7}$$

Substitute (B7) into the expression for $S(\boldsymbol{Y})$ in (B5),

$$S(\boldsymbol{Y}) = \frac{\left(\sum\limits_{j=3}^{4N}\mu_j y_j w_j\right)^2}{\mu_2 w_2^2} + \sum_{j=3}^{4N}\mu_j y_j^2. \tag{B 8}$$

However, the condition $\mu_2 \mathrm{d}I/\mathrm{d}c > 0$ leads to

$$\mu_2\frac{\mathrm{d}I}{\mathrm{d}c} = \mu_2\langle\nabla I(\mathscr{U}), \mathscr{U}_c\rangle = \mu_2\langle\mathrm{L}(\mathscr{U}, c)\,\mathscr{U}_c, \mathscr{U}_c\rangle > 0$$

or in terms of the spectral expansion for $\mathscr{U}_c$,

$$\mu_2^2 w_2^2 + \mu_2\sum_{j=3}^{4N}\mu_j w_j^2 > 0. \tag{B 9}$$

If $\mu_2 > 0$ it is clear from (B8) that $S(\boldsymbol{Y}) > 0$. If $\mu_2 < 0$ let $\mu_2 = -|\mu_2|$ then (B9) is equivalent to

$$\frac{-1}{|\mu_2| w_2^2} > \frac{-1}{\sum\limits_{j=3}^{4N}\mu_j w_j^2}. \tag{B 10}$$

Now substitute (B10) into the expression for $S(\boldsymbol{Y})$ in (B8) to find

$$S(\boldsymbol{Y}) = \frac{\left(\sum\limits_{j=3}^{4N}\mu_j y_j w_j\right)^2}{\mu_2 w_2^2} + \sum_{j=3}^{4N}\mu_j y_j^2 > -\frac{\left(\sum\limits_{j=3}^{4N}\mu_j y_j w_j\right)^2}{\sum\limits_{j=3}^{4N}\mu_j w_j^2} + \sum_{j=3}^{4N}\mu_j y_j^2 > 0,$$

where positivity of $S(\boldsymbol{Y})$ follows from the Cauchy–Schwartz inequality, completing the proof.

## Appendix C. The critical eigenvalue of $\mathrm{L}(\mathscr{U},c)$ and the bifurcation function $h$

In this Appendix it is shown that the critical eigenvalue $\mu_2(\mathscr{U},c)$ of $\mathrm{L}(\mathscr{U},c)$, the second variation of $\mathscr{F}(\mathscr{U},c)$, has the same sign as the trace of the second variation of the reduced functional $G(A_1,B_1;c)$ for $\|\mathscr{U}\|$ sufficiently small.

The idea is to partition both the vector $\mathscr{U}$ and the $4N\times 4N$ matrix $\mathrm{L}(\mathscr{U},c)$. Let

$$\mathscr{U}=(\boldsymbol{x},\boldsymbol{\Lambda}) \quad \text{with} \quad \boldsymbol{x}=\begin{pmatrix} A_1 \\ B_1 \end{pmatrix}\in\mathbb{R}^2 \quad \text{and} \quad \boldsymbol{\Lambda}\in\mathbb{R}^{4N-2}, \tag{C 1}$$

where $\boldsymbol{\Lambda}$ contains $C_1$, $D_1$ $A_2$, $B_2$, $C_2$, $D_2$, …, $A_N$, $B_N$, $C_N$ and $D_N$. Now partition the second variation of $\mathscr{F}(\mathscr{U},c)$ in a like manner:

$$\mathrm{L}(\mathscr{U},c)=\begin{bmatrix} \mathscr{F}_{xx} & \mathscr{F}_{\Lambda x}^T \\ \mathscr{F}_{\Lambda x} & \mathscr{F}_{\Lambda\Lambda} \end{bmatrix}, \tag{C 2}$$

where

$$\mathscr{F}_{xx}=\begin{bmatrix} \dfrac{\partial^2\mathscr{F}}{\partial A_1^2} & \dfrac{\partial^2\mathscr{F}}{\partial A_1\partial B_1} \\ \dfrac{\partial^2\mathscr{F}}{\partial B_1\partial A_1} & \dfrac{\partial^2\mathscr{F}}{\partial B_1^2} \end{bmatrix} \tag{C 3}$$

is a $2\times 2$ matrix, $\mathscr{F}_{\Lambda x}$ is the $(4N-2)\times 2$ matrix

$$\mathscr{F}_{\Lambda x}=\begin{pmatrix} \dfrac{\partial^2\mathscr{F}}{\partial\boldsymbol{\Lambda}\partial A_1} & \dfrac{\partial^2\mathscr{F}}{\partial\boldsymbol{\Lambda}\partial B_1} \end{pmatrix} \tag{C 4}$$

and $\mathscr{F}_{\Lambda\Lambda}$ is a square matrix of dimension $4N-2$ containing the second partial derivatives of $\mathscr{F}$ with respect to the elements of $\boldsymbol{\Lambda}$. The reason for the partition of L is that $\mathscr{F}_{\Lambda\Lambda}$ is invertible when $A_1$ and $B_1$ are sufficiently small since $\mathscr{F}_{\Lambda\Lambda}|_{A_1=B_1=0}$ has $4N-2$ positive eigenvalues, (cf. §3.2). The linear operator $\mathrm{L}(0,c_0)$ has two zero eigenvalues, one of which remains zero under perturbation due to the group orbit of solutions. It is the perturbation of the other zero eigenvalue that is of interest here. Denote it by $\mu_2(\mathscr{U},c)$ with $\mu_2(0,c_o)=0$.

Consider the characteristic equation for L,

$$\det[\mathrm{L}(\mathscr{U},c)-\mu\boldsymbol{I}]=0. \tag{C 5}$$

Let $\boldsymbol{I}_2$ be the identity on $\mathbb{R}^2$ and let $\widehat{\boldsymbol{I}}$ be the identity on $R^{4N-2}$, then (C5), using the decomposition (C2), is equivalent to

$$\left|\begin{pmatrix} \boldsymbol{I}_2 & -\mathscr{F}_{\Lambda x}^T(\mathscr{F}_{\Lambda\Lambda}-\mu\widehat{\boldsymbol{I}})^{-1} \\ \boldsymbol{0} & \widehat{\boldsymbol{I}} \end{pmatrix}\begin{pmatrix} \mathscr{F}_{xx}-\mu\boldsymbol{I}_2 & \mathscr{F}_{\Lambda x}^T \\ \mathscr{F}_{\Lambda x} & \mathscr{F}_{\Lambda\Lambda}-\mu\widehat{\boldsymbol{I}} \end{pmatrix}\right|=0$$

or

$$|\mathscr{F}_{\Lambda\Lambda}-\mu\widehat{\boldsymbol{I}}|\cdot|\mathscr{F}_{xx}-\mathscr{F}_{\Lambda x}^T(\mathscr{F}_{\Lambda\Lambda}-\mu\widehat{\boldsymbol{I}})^{-1}\mathscr{F}_{\Lambda x}-\mu\boldsymbol{I}_2|=0. \tag{C 6}$$

For $\mu$ sufficiently small (near a zero eigenvalue of $\mathrm{L}(0,c_0)$) the determinant $|\mathscr{F}_{\Lambda\Lambda}-\mu\widehat{\boldsymbol{I}}|$ is non-zero and the first factor in (C6) may be divided out. Note that the zero eigenvalue of $\mathrm{L}(0,c_0)$ due to symmetry is contained in the second factor of (C6) resulting in the identity

$$|\mathscr{F}_{xx}-\mathscr{F}_{\Lambda x}^T\mathscr{F}_{\Lambda\Lambda}^{-1}\mathscr{F}_{\Lambda x}|=0. \tag{C 7}$$

Define the $2\times 2$ matrix $\widehat{\mathscr{F}}_{xx}$ by

$$\widehat{\mathscr{F}}_{xx}=\mathscr{F}_{xx}-\mathscr{F}_{\Lambda x}^T\mathscr{F}_{\Lambda\Lambda}^{-1}\mathscr{F}_{\Lambda x} \tag{C 8}$$

and let

$$\mathscr{F}_{\Lambda x}^{T}\left((\mathscr{F}_{\Lambda\Lambda}-\mu\widehat{\boldsymbol{I}})^{-1}-\mathscr{F}_{\Lambda\Lambda}^{-1}\right)\mathscr{F}_{\Lambda x}=\mu\mathscr{E}(\mu), \tag{C 9}$$

where $\mathscr{E}(\mu)$ is a $2\times 2$ symmetric matrix with

$$\mathscr{E}(0)=\mathscr{F}_{\Lambda x}^{T}\mathscr{F}_{\Lambda\Lambda}^{-2}\mathscr{F}_{\Lambda x}\,.$$

Since $\mathscr{F}_{\Lambda x}=0$ when $A_1=B_1=0$ it follows that $\mathscr{E}(0)$ can be made as small as required by choosing $A_1^2+B_1^2$ sufficiently small. Using (C8) and (C9) the characteristic equation in (C6) simplifies to

$$0=|\widehat{\mathscr{F}}_{xx}-\mu(\boldsymbol{I}_2+\mathscr{E}(\mu))|=|(\boldsymbol{I}_2+\mathscr{E}(\mu))|\,|(\boldsymbol{I}_2+\mathscr{E}(\mu))^{-1}\widehat{\mathscr{F}}_{xx}-\mu\boldsymbol{I}_2| \tag{C 10}$$

which, for $\|\mathscr{E}(\mu)\|$ sufficiently small-leads to

$$\mu^2-\mathrm{Tr}\left\{(\boldsymbol{I}_2+\mathscr{E}(\mu))^{-1}\widehat{\mathscr{F}}_{xx}\right\}\mu+|(\boldsymbol{I}_2+\mathscr{E}(\mu))^{-1}\widehat{\mathscr{F}}_{xx}|=0\,.$$

Comparison of (C7) and (C8) shows that $|\widehat{\mathscr{F}}_{xx}|=0$. Therefore the expression for the critical eigenvalue $\mu_2$ is

$$\mu_2=\mathrm{Tr}\left\{(\boldsymbol{I}_2+\mathscr{E}(\mu))^{-1}\widehat{\mathscr{F}}_{xx}\right\}=\mathrm{Tr}\,\widehat{\mathscr{F}}_{xx}+\cdots\,. \tag{C 11}$$

When $\|\mathscr{E}(\mu)\|$ is sufficiently small (i.e. $A_1^2+B_1^2$ and $|\mu|$ sufficiently small)

$$\mathrm{sign}(\mu_2)=\mathrm{sign}(\mathrm{Tr}\widehat{\mathscr{F}}_{xx})\,. \tag{C 12}$$

It remains to show a relation between $\mathrm{Tr}(\widehat{\mathscr{F}}_{xx})$ and the reduced bifurcation equation $h(z,c,u,r)$. First note that $F(\mathscr{U},c)=H(\mathscr{U})-cI(\mathscr{U})$, with $\mathscr{U}$ decomposed as in (C1), and that $\nabla F(\mathscr{U},c)=0$. Solving the $4N-2$ equations $\partial\mathscr{F}/\partial\boldsymbol{\Lambda}=0$ for $\boldsymbol{\Lambda}$ as a function of $A_1$, $B_1$ and $c$ results in the identity

$$\frac{\partial\mathscr{F}}{\partial\boldsymbol{\Lambda}}(A_1,B_1,\boldsymbol{\Lambda}(A_1,B_1;c);c)=0\,. \tag{C 13}$$

Differentiate (C13) with respect to $A_1$ to obtain

$$\frac{\partial^2\mathscr{F}}{\partial\boldsymbol{\Lambda}\partial A_1}+\frac{\partial^2\mathscr{F}}{\partial\boldsymbol{\Lambda}^2}\frac{\partial\boldsymbol{\Lambda}}{\partial A_1}=0,$$

implying that

$$\frac{\partial\boldsymbol{\Lambda}}{\partial A_1}=-\mathscr{F}_{\Lambda\Lambda}^{-1}\frac{\partial^2\mathscr{F}}{\partial\boldsymbol{\Lambda}\partial A_1} \tag{C 14}$$

and similarly

$$\frac{\partial\boldsymbol{\Lambda}}{\partial B_1}=-\mathscr{F}_{\Lambda\Lambda}^{-1}\frac{\partial^2\mathscr{F}}{\partial\boldsymbol{\Lambda}\partial B_1}\,. \tag{C 15}$$

Recall the definition of $h(z,c,u,r)$ given in equation (2.48) (noting also (2.43) and (2.46)) and substitute $\boldsymbol{\Lambda}(A_1,B_1;c)$ into $\partial\mathscr{F}/\partial A_1=0$ and $\partial\mathscr{F}/\partial B_1=0$ to obtain

$$-2A_1h(z,c,u,r)=\frac{\partial\mathscr{F}}{\partial A_1}(A_1,B_1,\boldsymbol{\Lambda}(A_1,B_1;c);c)=0, \tag{C 16}$$

$$-2B_1h(z,c,u,r)=\frac{\partial\mathscr{F}}{\partial B_1}(A_1,B_1,\boldsymbol{\Lambda}(A_1,B_1;c);c)=0\,. \tag{C 17}$$

Differentiate (C16) with respect to $A_1$ and (C17) with respect to $B_1$ and use the fact

that $z = k(A_1^2 + B_1^2)$ and $h = 0$ along a solution branch:

$$-4k^2 A_1^2 h_z = \frac{\partial^2 \mathscr{F}}{\partial A_1^2} + \left(\frac{\partial^2 \mathscr{F}}{\partial \boldsymbol{\Lambda} \partial A_1}\right)^T \frac{\partial \boldsymbol{\Lambda}}{\partial A_1}, \tag{C 18}$$

$$-4k^2 B_1^2 h_z = \frac{\partial^2 \mathscr{F}}{\partial B_1^2} + \left(\frac{\partial^2 \mathscr{F}}{\partial \boldsymbol{\Lambda} \partial B_1}\right)^T \frac{\partial \boldsymbol{\Lambda}}{\partial B_1}. \tag{C 19}$$

Now add equations (C18) and (C19) and use (C14) and (C15):

$$-4z h_z = \frac{\partial^2 \mathscr{F}}{\partial A_1^2} - \left(\frac{\partial^2 \mathscr{F}}{\partial \boldsymbol{\Lambda} \partial A_1}\right)^T \mathscr{F}_{\boldsymbol{\Lambda}\boldsymbol{\Lambda}}^{-1} \left(\frac{\partial^2 \mathscr{F}}{\partial \boldsymbol{\Lambda} \partial A_1}\right) + \frac{\partial^2 \mathscr{F}}{\partial B_1^2} - \left(\frac{\partial^2 \mathscr{F}}{\partial \boldsymbol{\Lambda} \partial B_1}\right)^T \mathscr{F}_{\boldsymbol{\Lambda}\boldsymbol{\Lambda}}^{-1} \left(\frac{\partial^2 \mathscr{F}}{\partial \boldsymbol{\Lambda} \partial B_1}\right).$$

But recalling the definition of $\mathscr{F}_{xx}$ and $\mathscr{F}_{\boldsymbol{\Lambda}x}$ it is clear that the right-hand side of this expression is simply the trace of $\widehat{\mathscr{F}}_{xx}$. We have proved the following identity:

$$\operatorname{sign}(\mu_2) = -\operatorname{sign}(h_z),$$

for the sign of the critical eigenvalue of $\mathrm{L}(\mathscr{U}, c)$.

## REFERENCES


Benjamin, T. B. 1972 The stability of solitary waves. *Proc. R. Soc. Lond.* A**328**, 153–83.

Benjamin, T. B. 1984 Impulse, flow force and variational principles. *IMA J. Appl. Maths* **32**, 3–68.

Benjamin, T. B. & Bridges, T. J. 1997 Reappraisal of the Kelvin–Helmholtz problem. Part 1. Hamiltonian structure. *J. Fluid Mech.* **333**, 301–325 (referred to herein as I).

Benjamin, T. B. & Feir, J. E. 1967 The disintegration of wavetrains on deep water. Part 1. Theory. *J. Fluid Mech.* **27**, 417–430.

Bontozoglou, V. & Hanratty, T. 1988 Effects of finite depth and current velocity on large amplitude Kelvin–Helmholtz waves. *J. Fluid Mech.* **196**, 187–204.

Bridges, T. J. 1990 Bifurcation of periodic solutions near a collision of eigenvalues of opposite signature. *Math. Proc. Camb. Phil. Soc.* **108**, 575–601.

Bridges, T. J. 1991 Stability of periodic solutions near a collision of eigenvalues of opposite signature. *Math. Proc. Camb. Phil. Soc.* **109**, 375–403.

Bridges, T. J. 1994 Geometric aspects of degenerate modulation equations. *Stud. Appl. Maths* **91**, 125–151.

Bridges, T. J., Christodoulides, P. & Dias, F. 1995 Spatial bifurcations of interfacial waves when the phase and group velocities are nearly equal. *J. Fluid Mech.* **295**, 121–158.

Bridges, T. J. & Mielke, A. 1995 A proof of the Benjamin-Feir instability. *Arch. Rat. Mech. Anal.* **133**, 145–198.

Christodoulides, P. & Dias, F. 1994 Resonant capillary–gravity interacial waves. *J. Fluid Mech.* **265**, 303–343.

Deprit, A. & Henrard, J. 1968 A manifold of periodic orbits. *Adv. Astron. Astrophys.* **6**, 1–124.

Dias, F. & Bridges, T. J. 1994 Geometric aspects of spatially periodic interfacial waves. *Stud. Appl. Maths* **93**, 93–132.

Drazin, P. G. 1970 Kelvin–Helmholtz instability of finite amplitude. *J. Fluid Mech.* **42**, 321–35.

Drazin, P. G. & Reid, W. H. 1981 *Hydrodynamic Stability*. Cambridge University Press.

Eckhaus, W. & Iooss. G. 1989 Strong selection or rejection of spatially periodic patterns in degenerate bifurcations. *Physica* D **39**, 124–46.

Golubitsky, M. & Schaeffer, D. G. 1985 *Singularities and Groups in Bifurcation Theory, Vol. I.* Springer.

Grimshaw, R. H. J. & Pullin, D. I. 1985 Stability of finite-amplitude interfacial waves. Part 1. Modulational instability for small-amplitude waves. *J. Fluid Mech.* **160**, 297–315.

Hogan, S. J. 1980 Some effects of surface tension on steep water waves. Part 2. *J. Fluid Mech.* **96**, 417–445.

Holyer, J. Y. 1979 Large amplitude progressive interfacial waves. *J. Fluid Mech.* **93**, 433–48.

JILLIANS, W. J. 1989 The superharmonic instability of Stokes waves in deep water. *J. Fluid Mech.* **204**, 563–579.

JOHNSON, R. S. 1977 On the modulation of water waves in the neighborhood of $kh \approx 1.363$. *Proc. R. Soc. Lond.* A **357**, 131–141.

LONGUET-HIGGINS, M. S. 1978 The instability of gravity waves of finite amplitude in deep water. I. Superharmonics. *Proc. R. Soc. Lond.* A **360**, 471–488.

LONGUET-HIGGINS, M. S. & CLEAVER, R. P. 1994 Crest instabilities of gravity waves. Part 1. The almost highest wave. *J. Fluid Mech.* **258**, 115–29.

MADDOCKS, J. 1991 On the stability of relative equilibria. *IMA J. Appl. Maths.* **46**, 71–91.

MCLEAN, J. W. 1982 Instabilities of finite-amplitude water waves. *J. Fluid Mech.* **114**, 315–330.

MEER, J. C. VAN DER 1985 *The Hamiltonian Hopf Bifurcation.* Lecture Notes in Mathematics Vol. 1160, Springer.

MILES, J. W. 1986 Weakly nonlinear Kelvin–Helmholtz waves. *J. Fluid Mech.* **172**, 513–529.

NAYFEH, A. H. & SARIC, W. 1972 Nonlinear waves in Kelvin-Helmholtz flow. *J. Fluid Mech.* **55**, 311–327.

OH, Y. G. 1987 A stability theory for Hamiltonian systems. *J. Geom. Phys.* **4**, 163–182.

PULLIN, D. I. & GRIMSHAW, R. H. J. 1985 Stability of finite-amplitude interfacial waves. Part 2. Numerical results. *J. Fluid Mech.* **160**, 317–386.

ROBINET, J.-C. 1993 Etude numerique de l'instabilite de Kelvin-Helmholtz. *INLN Rep.*, Université de Nice.

SAFFMAN, P. G. 1985 The superharmonic instability of finite-amplitude water waves. *J. Fluid Mech.* **159**, 169–174.

SAFFMAN, P. G. 1992 *Vortex Dynamics.* Cambridge University Press.

TANAKA, M. 1983 The stability of steep gravity waves. *J. Phys. Soc. Japan* **52**, 2047–2055.

TANAKA, M. 1985 The stability of steep gravity waves, Part 2. *J. Fluid Mech.* **156**, 281–289.

TANAKA, M., DOLD, J. W., LEWY, M. & PEREGRINE, D. H. 1987 Instability and breaking of a solitary wave. *J. Fluid Mech.* **185**, 235–248.

THORPE, S. A. 1969 Experiments on the instability of stratified shear flows: immisciple fluids. *J. Fluid Mech.* **39**, 25–48.

THORPE, S. A. 1978 On the shape and breaking of finite amplitude internal gravity waves in a shear flow. *J. Fluid Mech.* **85**, 7–31.

TSUJI, Y. & NAGATA, Y. 1973 Stokes' expansion of internal deep-water waves to the fifth order. *J. Ocean. Soc. Japan* **29**, 61–69.

WEISSMAN, M. A. 1979 Nonlinear wave packets in the Kelvin–Helmholtz instability. *Phil. Trans. R. Soc. Lond.* A **290**, 639–685.

WHITHAM, G. B. 1974 *Linear and Nonlinear Waves.* Wiley-Interscience.

YUEN, H. C. 1984 Nonlinear dynamics of interfacial waves. *Physica* D **12**, 71–82.